

1 **Climatic Effects of 1950-2050 Changes in US Anthropogenic Aerosols - Part 2:**  
2 **Climate Response**

3  
4 **E. M. Leibensperger ([eleibens@mit.edu](mailto:eleibens@mit.edu))\***, L. J. Mickley, D. J. Jacob  
5 *School of Engineering and Applied Sciences, Harvard University, Cambridge, MA USA*

6 W.-T. Chen

7 *Jet Propulsion Laboratory, California Institute of Technology, Pasadena, CA USA*

8 J. H. Seinfeld

9 *Division of Chemistry and Chemical Engineering, California Institute of Technology,*  
10 *Pasadena, CA USA*

11 A. Nenes

12 *School of Earth & Atmospheric Sciences and School of Chemical & Biological*  
13 *Engineering, Georgia Institute of Technology, Atlanta, GA USA*

14 P. J. Adams

15 *Department of Civil & Environmental Engineering and Department Engineering &*  
16 *Public Policy, Carnegie Mellon University, Pittsburgh, PA USA*

17 D. G. Streets

18 *Argonne National Laboratory, Argonne, IL USA*

19 N. Kumar

20 *Electric Power Research Institute, Palo Alto, CA USA*

21 D. Rind

22 *NASA Goddard Institute for Space Studies, New York, NY USA*

23  
24 *\*Now at Department of Earth, Atmospheric and Planetary Sciences, Massachusetts*  
25 *Institute of Technology, Cambridge, MA USA*

26  
27 May 16, 2011  
28

28 **Abstract**

29 We investigate the climate response to US anthropogenic aerosol sources over the 1950  
30 to 2050 period by using the NASA GISS general circulation model (GCM) and  
31 comparing to observed US temperature trends. Time-dependent aerosol distributions are  
32 generated from the GEOS-Chem chemical transport model applied to historical emission  
33 inventories and future projections. Radiative forcing from US anthropogenic aerosols  
34 peaked in 1970-1990 and has strongly declined since due to air quality regulations. We  
35 find that the regional radiative forcing from US anthropogenic aerosols elicits a strong  
36 regional climate response, cooling the central and eastern US by 0.5-1.0°C on average  
37 during 1970-1990, with the strongest effects on maximum daytime temperatures in  
38 summer and autumn. Aerosol cooling reflects comparable contributions from direct and  
39 indirect (cloud-mediated) radiative effects. Absorbing aerosol (mainly black carbon) has  
40 negligible warming effect. Aerosol cooling reduces surface evaporation and thus  
41 decreases precipitation along the US east coast, but also increases the southerly flow of  
42 moisture from the Gulf of Mexico resulting in increased cloud cover and precipitation in  
43 the central US. Observations over the eastern US show a lack of warming in 1960-1980  
44 followed by very rapid warming since, which we reproduce in the GCM and attribute to  
45 trends in US anthropogenic aerosol sources. Present US aerosol concentrations are  
46 sufficiently low that future air quality improvements are projected to cause little further  
47 warming in the US (0.1°C over 2010-2050). We find that most of the potential warming  
48 from aerosol source controls in the US has already been realized over the 1980-2010  
49 period.

50 **1. Introduction**

51 Global mean surface temperatures increased by  $0.74 \pm 0.18^{\circ}\text{C}$  between 1906 and 2005  
52 due to increasing greenhouse gases (Trenberth et al., 2007). However, temperature trends  
53 on regional scales are more complicated. For example, the eastern US experienced a  
54 cooling between 1930 and 1990 (Fig. 1). The net cooling effect of anthropogenic aerosols  
55 is known to have mitigated some of the global warming from greenhouse gases (Hegerl et  
56 al., 2007), but the importance of aerosol cooling on temperature trends in the US has  
57 received little attention. As US aerosol sources are increasingly controlled to improve air  
58 quality, the associated cooling is undone resulting in accelerated warming (Andreae et al.,  
59 2005; Brasseur and Roeckner, 2005; Kloster et al., 2009; Mickley et al., submitted). Air  
60 quality improvement thus comes with climate consequences (Raes and Seinfeld, 2009).  
61 In Leibensperger et al. (submitted), we reconstructed and projected the aerosol trends and  
62 associated radiative forcing from US anthropogenic sources over the 1950-2050 period.  
63 US aerosol concentrations peaked in 1970-1990 and have decreased rapidly since. We  
64 use here a general circulation model (GCM) to study the associated climate response.

65  
66 Anthropogenic aerosols directly affect the climate system by scattering and absorbing  
67 solar radiation, and indirectly by altering cloud microphysical properties. Aerosol  
68 scattering cools and absorption warms the atmosphere, but both cause a reduction in  
69 surface solar radiation. Observations of surface solar radiation over the US show a  
70 widespread decrease over the 1950-1990 period followed by more recent increase  
71 (Liepert and Tegen, 2002; Long et al., 2009). These trends have been identified in clear  
72 and all-sky scenes, suggesting a role for both direct and indirect aerosol effects. These  
73 trends in surface solar radiation are qualitatively consistent with changes in aerosol  
74 sources (Streets et al., 2009), but cannot be entirely explained by anthropogenic aerosols  
75 (Liepert and Tegen, 2002; Long et al., 2009; Wild, 2009b).

76  
77 Aerosols are scavenged from the atmosphere by precipitation on a time scale of days, so  
78 that their radiative forcing is strongly localized over source regions (Schulz et al., 2006).  
79 A critical issue is whether the regional radiative forcing of aerosols elicits a  
80 correspondingly regional climate response. Observation-based studies have related

81 changes in surface solar radiation with other climate variables as a method of deducing  
82 the local effects of aerosol forcing. They show evidence that aerosols have lowered  
83 surface air temperature and temporarily offset greenhouse warming (Qian and Giorgi,  
84 2000; Wild et al., 2007; Ruckstuhl et al., 2008; Philipona et al., 2009), reduced the  
85 diurnal temperature range by dampening daily maximum temperatures (Liu et al., 2004b;  
86 Wild et al., 2007; Makowski et al., 2009), lowered evaporation rates (Peterson et al.,  
87 1995; Liu et al., 2004a; Roderick et al., 2007), and increased soil moisture (Robock et al.,  
88 2005).

89

90 Some GCM studies have found strong regional climate sensitivity to aerosols including in  
91 India (Menon et al., 2002; Wang et al., 2009a), southeast Asia (Chang et al., 2009; Zhang  
92 et al., 2009; Lee and Kim, 2010), the North Atlantic (Fischer-Bruns et al., 2009), and  
93 western US (Jacobson, 2008). However, other studies have found that aerosol radiative  
94 forcing elicits little regional climate response, and produces instead a global climate  
95 effect with patterns similar (but opposite in sign) to greenhouse gas forcing (Mitchell et  
96 al., 1995; Shindell et al., 2007; Levy et al., 2008; Shindell et al., 2008; Kloster et al.,  
97 2009). Mickley et al. (submitted) used a GCM to simulate the climate response of  
98 completely removing aerosols over the US and found a 0.4-0.6°C regional warming in  
99 the US with little effect elsewhere. Fischer-Bruns et al. (2010) investigated the climate  
100 impacts of removing North American aerosols and found a 1.0-1.5°C summer warming  
101 in surface air over the US and North Atlantic Ocean. The same study also found a 1.5-  
102 2.0°C warming of the Arctic in winter.

103

104 There is strong motivation for air quality agencies to decrease aerosol concentrations to  
105 improve public health. Better understanding of the associated climate response is  
106 necessary. The US is of particular interest in this regard because aerosol concentrations  
107 rose in the 20<sup>th</sup> century, peaked in the 1980s, and have been decreasing rapidly since due  
108 in large part to a 56% reduction of SO<sub>2</sub> emissions between 1980 and 2008 (US EPA,  
109 2010). Here we use the 1950-2050 time series of US aerosol trends and radiative forcing  
110 from Leibensperger et al. (submitted) to conduct 1950-2050 transient-climate simulations  
111 with the NASA Goddard Institute for Space Studies (GISS) GCM 3 (Rind et al., 2007).

112 Our objective is to investigate the regional climate effects of historical and projected  
113 changes in US anthropogenic aerosol sources. An important advance compared to  
114 previous work is the use of a realistic evolution of aerosol sources.

115

## 116 **2. Methods**

117 We conduct sensitivity simulations with the GISS GCM 3 to study the evolving 1950-  
118 2050 climate response to changing US anthropogenic aerosol sources. The GCM uses  
119 archived global 3-D monthly mean concentrations of different aerosol components from  
120 the GEOS-Chem chemical transport model (CTM) with time-dependent emissions based  
121 on historical data and future projections. The CTM simulations are described by  
122 Leibensperger et al. (submitted) and a brief summary is given below.

123

### 124 **2.1 Aerosol Simulations**

125 We conduct a 2-year GEOS-Chem simulation of coupled ozone-NO<sub>x</sub>-VOC-aerosol  
126 chemistry (<http://geos-chem.org>; Bey et al., 2001; Park et al., 2004) for each decade  
127 between 1950 and 2050. The first year is used as model initialization. Monthly mean fine  
128 aerosol concentrations are archived from the second year for use in the GCM including  
129 sulfate-nitrate-ammonium (SNA), primary organic aerosol (POA), secondary organic  
130 aerosol (SOA), and black carbon (BC) (Park et al., 2006; Liao et al., 2007). Simulations  
131 for all years use the same assimilated meteorological data from 2000-2001 so that  
132 changes in concentrations over the 1950-2050 period are due to emissions only. The  
133 meteorological data are from the NASA Goddard Earth Observing System (GEOS)-4  
134 with 1°x1.25° horizontal resolution, 55 vertical levels, and 6-hour temporal resolution (3-  
135 hour for surface variables and mixing depths). The horizontal resolution is degraded to  
136 2°x2.5° for input to GEOS-Chem. The effect of US anthropogenic sources is determined  
137 by parallel sensitivity simulations for the 1950-2050 period with zero US anthropogenic  
138 emissions of SO<sub>2</sub>, NO<sub>x</sub>, POA, and BC. “Anthropogenic” here includes fuel and industrial  
139 sources but not open fires.

140

141 We use 1950-1990 global anthropogenic emissions of SO<sub>2</sub> and NO<sub>x</sub> from EDGAR Hyde  
142 1.3 (van Aardenne et al., 2001) and 2000 emissions from EDGAR 3.2 FT (Olivier and

143 Berdowski, 2001). Historical emissions of BC and POA are from Bond et al. (2007).  
144 Emissions past 2000 are calculated using growth factors derived from the Integrated  
145 Model to Assess the Greenhouse Effect (IMAGE; Streets et al., 2004) following the  
146 IPCC A1B scenario (Nakićenović and Swart, 2000). As in Fiore et al. (2002) and Wu et  
147 al. (2008), growth factors are calculated for different countries and fuel types (fossil fuel  
148 and biofuel). Ammonia emissions are from Bouwman et al. (1997) as modified by Park et  
149 al. (2004), except for East Asia (Streets et al., 2003). Additional sources include  
150 climatological biomass burning (Duncan et al., 2003), fertilizer (Wang et al., 1998),  
151 aircraft (Chin et al., 2000), the biosphere, volcanoes, and lightning. See Leibensperger et  
152 al. (submitted) for more detail.

153

## 154 **2.2 Climate Simulations**

155 We conduct transient climate simulations with the GISS GCM 3 using a horizontal  
156 resolution of  $4^\circ \times 5^\circ$  and 23 vertical levels that extend from the surface to 0.002 hPa.  
157 GISS GCM 3 shares a common history with another NASA GISS GCM, Model E  
158 (Schmidt et al., 2006), but the two differ in their parameterizations of gravity wave drag,  
159 convection, and the boundary layer (Rind et al., 2007). GISS GCM 3 has been previously  
160 used in studies investigating air quality-climate interactions (Leibensperger et al., 2008;  
161 Wu et al., 2008; Pye et al., 2009; Chen et al., 2010; Mickley et al., submitted), tracer  
162 transport (Rind et al., 2007), climate response to solar forcing (Rind et al., 2008), and  
163 stratospheric ozone-climate interactions (Rind et al., 2009a; Rind et al., 2009b). The  
164 model contains a Q-flux ocean, in which monthly oceanic heat transports are held  
165 constant but sea surface temperature and sea ice coverage are allowed to respond to  
166 energy exchange with the atmosphere (Hansen et al., 1988). We calculate ocean heat  
167 transport using equilibrium climate simulations forced with observed sea surface  
168 temperature (SST) and sea ice distributions for 1946-1955 (Rayner et al., 2003),  
169 following the method outlined by Hansen et al. (1988).

170

171 Archived 3-D monthly mean aerosol concentrations are imported from GEOS-Chem to  
172 compute the aerosol direct effect. Concentrations are interpolated between decadal time  
173 slices. Aerosol optical properties are calculated assuming an internal mixture. Following

174 Chung and Seinfeld (2002) and Liao et al. (2004), we assume a standard gamma aerosol  
175 size distribution with an effective dry radius of 0.3  $\mu\text{m}$  and area-weighted variance of 0.2.  
176 Optical properties of the internal mixture are calculated using the volume-weighted mean  
177 of the refractive indices of the individual components. The resulting direct forcing from  
178 US anthropogenic aerosol sources in 1980 (peak aerosol loading) is only  $-0.07 \text{ W m}^{-2}$   
179 globally but  $-2.0 \text{ W m}^{-2}$  over the eastern US (Leibensperger et al., submitted). Dust and  
180 sea salt aerosols are considered externally mixed and held constant for 1950-2050 at the  
181 climatological radiative forcing values of Hansen et al. (2002).

182

183 Aerosol indirect radiative effects are computed following the approach previously  
184 implemented by Chen et al. (2010) in the GISS GCM 3. This includes the first indirect  
185 effect (cloud albedo) and the second indirect effect (cloud lifetime) on liquid stratiform  
186 clouds only. Aerosol mass concentrations affect the cloud droplet number concentration  
187  $N_c$  ( $\text{m}^{-3}$ ), which in turn determines the effective radius of cloud droplets and the rate of  
188 autoconversion to precipitation. We calculate  $N_c$  from the archived GEOS-Chem aerosol  
189 mass distributions using the method of Chen et al. (2010):

190

$$\log N_c = A + B \log m_i \quad (1)$$

191

192 where  $m_i$  is the molar concentration of dissolved aerosol ions ( $\text{mol m}^{-3}$ ) and  $A$  and  $B$  are  
193 gridded 3-D monthly mean coefficients derived from detailed simulations of aerosol  
194 microphysics and activation within the GCM (Adams and Seinfeld, 2002; Nenes and  
195 Seinfeld, 2003; Fountoukis and Nenes, 2005; Pierce and Adams, 2006). Cloud optical  
196 depth scales as the inverse of the area-weighted mean effective radius  $r_e$  of the cloud  
197 droplet size distribution (Del Genio et al., 1996). We obtain  $r_e$  from:

$$r_e = \kappa^{-\frac{1}{3}} \left[ \frac{3L}{4\pi N_c} \right]^{\frac{1}{3}} \quad (2)$$

198

199 where  $L$  is the liquid water content of the cloud ( $\text{cm}^3$  water per  $\text{cm}^{-3}$  air), and  $\kappa$  is a  
200 constant (0.67 over land, 0.80 over ocean; Martin et al., 1994) that relates the volume-  
201 weighted mean and area-weighted mean radii. Autoconversion rates are calculated using

202 the parameterization of Khairoutdinov and Kogan (2000), which fits results from an  
203 explicit microphysical model:

204

$$\frac{dq_l}{dt} = -1350 \gamma q_l^{2.47} N_c^{-1.79} \quad (2)$$

205

206 where  $q_l$  is the cloudwater mass content ( $\text{kg kg}^{-1}$ ). Hoose et al. (2008) and Chen et al.  
207 (2010) added the tuning parameter  $\gamma$  in order to retain GCM climate equilibrium. We find  
208 that a  $\gamma$  value of 12 retains top-of-atmosphere (TOA) radiative balance in a climate  
209 equilibrium simulation for 1950 conditions including fixed SST and sea ice  
210 (Leibensperger et al., submitted).  $\gamma = 12$  is consistent with the recent results of Morales  
211 and Nenes (2010), who found that autoconversion rates can be underestimated by a factor  
212 of 2 to 10 when models use gridbox-scale values of  $N_c$ .

213

214 Two sets of control simulations were conducted. The first includes only the direct  
215 radiative forcing from aerosols, using the imported aerosol concentrations from GEOS-  
216 Chem. The second additionally imports  $N_c$  as calculated in Eq. 1 to account for the  
217 aerosol indirect effects. Sensitivity simulations were conducted relative to each of these  
218 controls using aerosol and  $N_c$  fields from the GEOS-Chem simulations with US  
219 anthropogenic sources of  $\text{SO}_2$ ,  $\text{NO}_x$ , POA, and BC shut off. Differences between the  
220 control and sensitivity simulations then measure the climate response to US  
221 anthropogenic sources through the direct and indirect effects of aerosols.

222

223 Each set of simulations consists of a five-member ensemble conducted from 1950 to  
224 2050 using the natural and greenhouse gas forcing described by Hansen et al. (2002).  
225 Future greenhouse gas concentrations follow the IPCC SRES A1B scenario with  $\text{CO}_2$ ,  
226  $\text{N}_2\text{O}$ , and  $\text{CH}_4$  reaching 522, 0.350, and 2.40 ppm, respectively, by 2050. Initiating  
227 climate simulations from 1950 equilibrium conditions neglects the small radiative  
228 imbalance that occurred at that time. A previous study with the GISS GCM using the  
229 same climate forcing as here (except for tropospheric aerosols) found the Earth to be out  
230 of radiative balance by  $+0.18 \text{ W m}^{-2}$  for 1951 conditions (Sun and Hansen, 2003). This

231 suggests that our simulations underestimate post-1950 global warming by approximately  
232 0.1°C, a small effect that does not impact our assessment of the climate response to US  
233 anthropogenic aerosols since it is common to both the control and sensitivity simulations.  
234

235 We conducted an additional sensitivity simulation to isolate the climate effects of US  
236 anthropogenic sources of BC. This simulation uses the sulfate, nitrate, POA, and SOA  
237 distributions from the control simulation, but no BC emission from US anthropogenic  
238 sources. Results indicate that the climate effects of US anthropogenic BC are small and  
239 indistinguishable from interannual variability. This is consistent with the weak radiative  
240 forcing from US anthropogenic BC (+0.4 W m<sup>-2</sup> over the eastern US for 1970-1990).  
241 Previous studies have shown a significant climate response in Asia where BC radiative  
242 forcing is greater (Menon et al., 2002; Wang et al., 2009), but this region has larger BC  
243 emissions. We do not discuss this simulation further.  
244

245 We test the statistical significance of all our results using a modified version of Student's  
246 t-test to account for serial correlation (Zwiers and von Storch, 1995). Results presented  
247 here are significant at the 95<sup>th</sup> percentile and represent the mean of ensemble members  
248 unless specified.  
249

### 250 **3. Climate Response to US Anthropogenic Aerosols**

#### 251 **3.1 Radiation**

252 Figure 2 shows the annual mean change in net TOA and surface solar radiation due to the  
253 direct and indirect radiative effects of US anthropogenic aerosols in 1970-1990, the  
254 period when US aerosol loadings were at their peak. These differ from the radiative  
255 forcings reported by Leibensperger et al. (submitted) in that they include the effects of  
256 climate response, such as changes in cloud cover. We find that the radiative effect is  
257 strongly concentrated over the eastern US, and define a mid-Atlantic US region boxed in  
258 Fig. 2 where the effect is maximum. The annual mean TOA radiative effect averages -6  
259 W m<sup>-2</sup> over that region, whereas the global TOA radiative effect is only -0.08 W m<sup>-2</sup>.  
260

261 The bottom panels of Fig. 2 show the 1950-2050 time series of the TOA and surface  
262 radiative effects from US anthropogenic aerosol sources over the mid-Atlantic region.  
263 Results are shown for the direct effect only and for the sum of direct and indirect effects.  
264 The magnitudes and trends of the direct effect match closely the corresponding  
265 instantaneous radiative forcings computed in Leibensperger et al. (submitted) (squares in  
266 Fig. 2). The indirect effect is comparable in magnitude to the direct effect. Sulfate is the  
267 largest contributor to US anthropogenic aerosol forcing (Leibensperger et al., submitted).  
268 We see from Fig. 2 that the radiative perturbations largely follow the evolution of SO<sub>2</sub>  
269 sources: increase until 1980 and rapid decrease afterward. Changes level off after 2020,  
270 by which time SO<sub>2</sub> emissions are 80% lower than their 1980 peak.

271  
272 The surface radiative effects in Fig. 2 are about 50% larger than the TOA effects due to  
273 aerosol absorption. Liepert and Tegen (2002) used six observation sites east of 95°W  
274 (downward triangles in Fig. 1) from the National Solar Radiation Database (NSRDB;  
275 [http://rredc.nrel.gov/solar/old\\_data/nsrdb/](http://rredc.nrel.gov/solar/old_data/nsrdb/)) to estimate a clear-sky trend in surface solar  
276 radiation of -7 W m<sup>-2</sup> between 1961 and 1990 that they attributed to the aerosol direct  
277 effect. Long et al. (2009) calculated an observed 1996-2007 increase in surface solar  
278 radiation of +5 W m<sup>-2</sup> (clear sky) and +8 W m<sup>-2</sup> (all sky) averaged over 11 Department of  
279 Energy Atmospheric Radiation Measurement (ARM) and National Oceanic and  
280 Atmospheric Administration (NOAA) US Surface Radiation Budget (SURFRAD) sites  
281 (upward triangles in Fig. 2). However, and as previously noted (Liepert and Tegen, 2002;  
282 Long et al., 2009; Wild, 2009a, b), we find that anthropogenic aerosols cannot explain the  
283 magnitude of the observed surface radiation trends. Sampling our control simulation at  
284 the six sites analyzed by Liepert and Tegen (2002), we find a simulated all-sky decrease  
285 of surface solar radiation of 1.1 W m<sup>-2</sup> between 1961 and 1990 due to the aerosol direct  
286 effect, much smaller than the observed value. Conversion of our all-sky trend to the clear-  
287 sky value would not reconcile the difference. Similarly, our control simulation  
288 underestimates the 1996-2007 all-sky increase of Long et al. (2009) (+2.4 W m<sup>-2</sup> vs. +8  
289 W m<sup>-2</sup>).

290

291 We previously showed that our simulated aerosol trends over the US are in good  
292 agreement with observations, at least for 1980-present when data are available  
293 (Leibensperger et al., submitted). The observed surface solar radiation trends thus seem  
294 much larger than can be explained from aerosol trends. The 1961-1990 NSRDB surface  
295 solar radiation data suffer from inconsistent data quality, but the more recent  
296 measurements presented by Long et al. (2009) have consistent annual calibration and  
297 daily performance monitoring. The cause of the model-observation discrepancy is unclear  
298 but suggests observed trends in surface radiation as cannot be solely driven by aerosols.  
299

### 300 **3.2 Temperature**

301 Figure 3 shows the annual mean temperature changes in surface air and at 500 hPa due to  
302 the direct and indirect effects of US anthropogenic aerosol sources over the 1970-1990  
303 period when US anthropogenic aerosol forcing was at its peak. Changes in surface air  
304 temperature are largest in the eastern US (0.5-1.0°C), collocated with the maximum  
305 radiative effect (Fig. 2). The cooling influence of US anthropogenic aerosols extends over  
306 much of the Northern Hemisphere, but beyond the US and North Atlantic Ocean it is only  
307 marginally significant against modeled interannual variability. The annual mean cooling  
308 averages 0.1°C for the Northern Hemisphere and 0.05°C for the Southern Hemisphere.  
309

310 As pointed out in the Introduction, some GCM studies find a strong spatial correlation  
311 between regional radiative forcing and climate response (as is shown here) while others  
312 do not. The reason is not clear and warrants a dedicated GCM intercomparison in the  
313 future. A contributing factor may be the magnitude and spatial distribution (horizontal  
314 and vertical) of the forcing. Larger, more distributed forcings may elicit more a global  
315 response. A recent study by Fisher-Bruns et al. (2010) of climate sensitivity to North  
316 American anthropogenic aerosol finds a strong Arctic climate response that is not  
317 apparent in our work.

318

319 Cooling is more diffuse at higher altitudes, reflecting the faster transport of heat (Fig. 3,  
320 top). At 500 hPa, the largest cooling is 0.3°C over the eastern US and North Atlantic  
321 Ocean. Statistically significant cooling covers more of the Northern Hemisphere at 500

322 hPa than at the surface. Annual mean cooling at 500 hPa averages  $0.1^{\circ}\text{C}$  for the Northern  
323 Hemisphere and  $0.02^{\circ}\text{C}$  for the Southern Hemisphere, similar to the hemispheric changes  
324 in surface air temperature. Cooling is even more diffuse at 300 hPa (not shown), but  
325 Northern Hemisphere cooling is similarly  $0.1^{\circ}\text{C}$ .

326

327 Figure 4 shows the surface air cooling due to US anthropogenic aerosols for the 1970-  
328 1990 period for the simulations including only the aerosol direct effect (top) and the  
329 combination of direct and indirect effects (bottom), focusing on the US. The bottom  
330 panel is a zoomed version of the bottom panel of Fig. 3. Significant cooling extends over  
331 much of the US even when the aerosol direct effect alone is considered. The magnitude  
332 of the cooling doubles when the indirect effects are included but the spatial patterns are  
333 similar. Thus the significance and localization of the US cooling due to US anthropogenic  
334 aerosol sources is not contingent on the indirect effects, which are far more uncertain  
335 than the direct effect. Cooling is strongest in the Midwest, shifted westward relative to  
336 the surface and TOA radiative effects shown in Fig. 2. This is due to hydrological factors  
337 and is discussed further in Section 3.3.

338

339 Figure 5 shows seasonal statistics of the effects of US anthropogenic aerosols on surface  
340 air temperatures in the mid-Atlantic US (boxed region in Fig. 2). The change in surface  
341 air temperature is largest in summer and autumn, with regionally averaged cooling of  
342 more than  $1.0^{\circ}\text{C}$  in autumn. Aerosol radiative forcing is largest in summer when solar  
343 radiation is strongest. The larger surface air temperature changes in autumn reflect the  
344 drier conditions so that less of the radiative effect is buffered by changes in surface  
345 evaporation (latent heat flux).

346

347 Figure 5 also presents the changes in extreme temperatures. We find that aerosol cooling  
348 has a larger effect on daily maximum than daily minimum temperatures, in all seasons, as  
349 expected since the forcing is due to scattering of solar radiation. The cooling is largest  
350 during heat waves of summer and autumn (95<sup>th</sup> percentile daily maximum temperatures,  
351 corresponding to the 5 hottest days of each season). These heat waves occur under cloud  
352 free conditions when the aerosol direct effect is especially effective. We find that the

353 warmest days are cooler by 1.0°C in summer and 1.3°C in autumn. The coldest nights of  
354 each season (5<sup>th</sup> percentile daily minimum temperatures) are least sensitive to aerosols  
355 except in winter when they are typically associated with synoptic-scale clear-sky  
356 conditions.

357

358 The model pattern of aerosol-driven cooling over the US in Fig. 4 is remarkably similar  
359 to the observed 1930-1990 trend in surface air temperature shown in Fig. 1. The largest  
360 area of cooling in the central US has previously been referred to as a “warming hole”  
361 (Pan et al., 2004; Kunkel et al., 2006). Previous GCM studies have associated this  
362 warming hole with variations in SSTs in the tropical Pacific (Robinson et al., 2002;  
363 Kunkel et al., 2006; Wang et al., 2009b). Kunkel et al. (2006) additionally point out a  
364 strong association between the observed variability of North Atlantic SSTs and central  
365 US surface temperatures. Our results indicate that the warming hole could be due to US  
366 anthropogenic aerosols, as SO<sub>2</sub> anthropogenic emissions in 1930 were only 60% of those  
367 in 1980. We find that US anthropogenic aerosols lower SSTs in the North Atlantic region  
368 outlined by Kunkel et al. (2006) by up to -0.3°C. Lower SSTs over the North Atlantic  
369 enhance the anticyclonic transport of marine air over the Gulf Coast of the US,  
370 magnifying the cooling as discussed below. The climate response to changes in SSTs is  
371 known to lag

372

### 373 **3.3 Hydrology and Dynamics**

374 Aerosols affect the hydrological cycle by reducing evaporation (due to reduced surface  
375 solar radiation) and by altering cloud cover and precipitation. Figure 6 shows the annual  
376 mean response of evaporation, precipitation, soil moisture availability, and cloud cover to  
377 US anthropogenic aerosols for the 1970-1990 period. The changes shown in Fig. 6 are for  
378 the total aerosol effect (direct + indirect), but similar responses with less statistical  
379 significance are found when only the aerosol direct effect is considered.

380

381 Reduced solar radiation at the surface decreases annual mean evaporation rates in the  
382 eastern US and the North Atlantic (Fig. 6a). The change is greatest in summer, when  
383 evaporation along the eastern seaboard decreases by up to 0.4 mm day<sup>-1</sup>. As mentioned in

384 Section 3.2, the decrease in latent heat flux associated with lower evaporation rates acts  
385 as a buffer to surface temperature changes, reducing the magnitude of aerosol cooling.  
386 We find that US anthropogenic aerosols decrease latent heat fluxes much more in  
387 summer ( $6.6 \text{ W m}^{-2}$  for 1970-1990 averaged over mid-Atlantic US) than in autumn ( $0.6$   
388  $\text{W m}^{-2}$ ), reflecting the greater availability of soil moisture in summer. In contrast to the  
389 general decrease in evaporation rates over the US, we find an increase in the south-  
390 central region. This is due to changes in soil moisture as discussed below.

391

392 The reduction in evaporation in the eastern US results in a decrease of downwind  
393 precipitation along the eastern seaboard (Fig. 6b). The decrease in precipitation is  
394 additionally promoted by the aerosol cloud lifetime effect (second aerosol indirect effect),  
395 which reduces the precipitation efficiency of clouds. The cloud lifetime effect is applied  
396 in the model to liquid stratiform clouds only, and this appears to be the dominant cause  
397 for the increase in eastern US cloud cover in Fig. 6c. We find little net change in moist  
398 convective cloud cover.

399

400 In contrast to the general slowdown of the hydrological cycle over the US, we find that  
401 evaporation and precipitation increase in the south central US. This is mostly driven by a  
402 summertime aerosol-induced change in circulation. Figure 7 shows the effect of US  
403 anthropogenic aerosols on 850 hPa geopotential heights in summer. Aerosols cool the  
404 North Atlantic (Fig. 2), strengthening the Bermuda High and thus the onshore flow of  
405 marine air from the Gulf of Mexico that is the principal source of moisture for the central  
406 and eastern US in summer. This enhances cloud cover, precipitation, and soil moisture  
407 over the south-central US (Fig. 6). A similar increase in central US precipitation due to  
408 anthropogenic sulfate was presented but not discussed by Jones et al. (2007). Increased  
409 cloud cover in the central US due to anthropogenic aerosols explains the particularly  
410 strong radiative and surface cooling effects in that region (Figs. 2 and 3). This is  
411 consistent with previous observational studies of the US warming hole which found it to  
412 be associated with additional moisture from the Gulf of Mexico causing enhanced  
413 evapotranspiration (Pan et al., 2004) and cloud cover (Robinson et al., 2002). Our work

414 suggests that US anthropogenic aerosols may be the drivers of changes in circulation  
415 causing central US cooling.

416

#### 417 **4. Aerosol effects on 1950-2050 trends in US surface air temperature**

418 Our analysis of the climate effects of US anthropogenic aerosols has focused so far on the  
419 1970-1990 period when the US aerosol loading was the largest. Leibensperger et al.  
420 (submitted) presented a detailed analysis of US anthropogenic aerosol trends for the  
421 1950-2050 period. US aerosol loading (and corresponding radiative forcing) increased  
422 from 1950 to 1980, decreased since then, and is projected to continue decreasing in the  
423 future (Fig. 2). Most of the anthropogenic aerosol radiative forcing is due to sulfate  
424 produced by oxidation of SO<sub>2</sub>. Emissions of SO<sub>2</sub> in the US decreased by 56% from their  
425 peak in 1980 to 2008 according to EPA (2010) and this is verified by observed trends in  
426 sulfate wet deposition (Leibensperger et al., submitted). US sources of SO<sub>2</sub> and other  
427 aerosol precursors in the IPCC A1B scenario are projected to continue to decrease until  
428 2020 and then level off.

429

430 Figure 8 shows the 1950-2050 simulated cooling trends over the mid-Atlantic US due to  
431 US anthropogenic aerosol sources. Cooling increased from -0.3°C in the 1950s to -  
432 0.65°C in the 1970s, remained flat until 1995, and decreased back to -0.3°C by 2010.  
433 Further decrease in aerosol cooling is projected over the coming decades but at a much  
434 slower rate, to -0.2°C by 2030. This trend in cooling is well correlated with the model  
435 trend in US aerosol sources (Leibensperger et al., submitted). The corresponding  
436 sensitivity of mid-Atlantic US surface air temperatures to regional aerosol forcing is  
437 0.09°C / W m<sup>-2</sup>. This is an order of magnitude smaller than the global climate sensitivity  
438 parameter of 0.76°C / W m<sup>-2</sup> for the GISS GCM 3 derived from doubled CO<sub>2</sub> simulations  
439 (Rind et al., 2007), as would be expected from the horizontal transport of heat. Still, we  
440 find that the large localized forcing elicits a strong regional climate response.

441

442 The trend of aerosol cooling over the mid-Atlantic US in Fig. 8 implies that most of the  
443 0.5°C warming over the US expected between 1980 and 2050 from aerosol decreases has  
444 in fact already been realized by 2010. This 1980-2010 warming trend in the model can be

445 compared to the observational record. Figure 9 shows the observed (GISTEMP;  
446 <http://data.giss.nasa.gov/gistemp/>) 1950-2010 time series of surface air temperature  
447 anomalies over the mid-Atlantic US in comparison to the control model simulation and to  
448 the sensitivity simulation with no US anthropogenic aerosol sources. Anomalies are  
449 relative to the 1951-1980 means in the observations and the control simulation and have  
450 been filtered by a 15-year moving average. Observed and simulated trends for different  
451 time periods are summarized in Table 1.

452

453 The observations show no significant warming between 1960 and 1979 ( $+0.01 \pm 0.20$  °C  
454  $\text{decade}^{-1}$ ). Our control simulation, which incorporates US anthropogenic aerosols,  
455 reproduces this result ( $-0.02 \pm 0.20$  °C  $\text{decade}^{-1}$ ). The simulation without US  
456 anthropogenic aerosols, however, produces significant warming over the period ( $+0.30 \pm$   
457  $0.19$  °C  $\text{decade}^{-1}$ ). We conclude that the increasing abundance of US anthropogenic  
458 aerosols effectively offset greenhouse warming before 1980.

459

460 Anthropogenic aerosol sources in the US peaked in 1980 and declined afterward. Fig. 9  
461 shows significant observed warming over the eastern US for the 1980-2009 period ( $+0.21$   
462  $\pm 0.20$  °C  $\text{decade}^{-1}$ ), in contrast to the 1960-1979 period when aerosol concentrations were  
463 increasing. Our control simulation reproduces this result, with a warming rate of  $+0.41 \pm$   
464  $0.08$  °C  $\text{decade}^{-1}$  for the 1980-2009 period. The sensitivity simulation without US  
465 anthropogenic aerosols shows slower warming ( $+0.30 \pm 0.10$  °C  $\text{decade}^{-1}$ ), which  
466 represents a continuation of the 1960-1979 trend due to greenhouse warming. The larger  
467 trend in the control simulation reflects the increasing trend of positive radiative forcing  
468 due to loss of the aerosol radiation shield. Beyond 2010 the rate of warming in the control  
469 simulation eases and eventually approaches that of the sensitivity simulation with no US  
470 anthropogenic aerosol sources.

471

## 472 **5. Conclusions**

473 Aerosol concentrations over the US peaked in the 1970-1990 period, have decreased  
474 rapidly since, and are projected to continue decreasing in the future as a result of air  
475 quality regulations to protect public health. We used a general circulation model (GISS

476 GCM 3) in a 1950-2050 transient-climate simulation to study the regional climate  
477 response to this time-dependent regional aerosol radiative forcing. Our goal was to  
478 determine how aerosol trends have contributed to recent climate trends over the US and  
479 to examine the climate consequences of further US aerosol reductions in the future.

480

481 We computed aerosol trends over the 1950-2050 period by using the GEOS-Chem  
482 chemical transport model (CTM) applied to historical emission inventories (1950-2000)  
483 and to future emission projections from the IPCC A1B scenario. Historical trends were  
484 evaluated with wet deposition and aerosol concentration data over the US. This work was  
485 described in Leibensperger et al. (submitted). Here we used the archived aerosol trends  
486 from GEOS-Chem to drive the transient-climate simulations in the GISS GCM 3. We  
487 conducted control simulations for 1950-2050 including our best estimates of greenhouse  
488 and aerosol radiative forcing, considering either the direct aerosol radiative forcing only  
489 or the combination of direct and indirect aerosol radiative forcings. Sensitivity  
490 simulations were conducted for both cases with US anthropogenic aerosol sources shut  
491 off. The climate response to US anthropogenic aerosol sources was diagnosed by  
492 difference between the control and sensitivity simulations. 5-member ensembles of  
493 simulations were conducted to test statistical significance.

494

495 We began by examining the climatic effects of US anthropogenic aerosol sources in  
496 1970-1990, when these sources were at their peak. During that period, the direct and  
497 indirect effects of US anthropogenic aerosols decreased top-of-atmosphere (TOA)  
498 radiation by up to  $8 \text{ W m}^{-2}$  over the eastern US ( $5 \text{ W m}^{-2}$  from the direct effect alone).  
499 Surface radiation over the mid-Atlantic US (boxed region of Fig. 2) decreased by  $2 \text{ W m}^{-2}$   
500 from 1950 to 1970 (“dimming”), remained flat from 1970 to 1990, and then increased  
501 by  $4 \text{ W m}^{-2}$  from 1990 to 2010 (“brightening”). These surface radiation trends in the  
502 model are qualitatively consistent with observed trends but much weaker. Considering  
503 that the model reproduces well the observed 1980-2010 aerosol trends in the US  
504 (Leibensperger et al., submitted), it appears that the observed dimming/brightening trends  
505 are much larger than can be explained from aerosols.

506

507 We find that US anthropogenic aerosols in 1970-1990 cooled the central and eastern US  
508 by 0.5-1.0°C on an annual mean basis. Half of this cooling is from the direct aerosol  
509 radiative effect and half is from indirect effects. The cooling is strongest in summer and  
510 autumn, and strongest during heat waves. Daily maximum temperatures on the hottest  
511 autumn days are lowered by 1.3°C. Our results are consistent with observations that show  
512 that the eastern US had a steady or cooling temperature trend from 1930 to 1980. This  
513 cooling anomaly in the observations has been reported previously as a “warming hole”  
514 (Pan et al., 2004; Kunkel et al., 2006). It has been attributed in these studies to sea surface  
515 temperature (SST) anomalies but we attribute it here to the effect of US anthropogenic  
516 aerosols.

517

518 We find that US anthropogenic aerosols generally slow down the hydrological cycle in  
519 the eastern US by reducing evaporation. This decreases precipitation along the east coast  
520 by up to 0.2 mm day<sup>-1</sup> on an annual mean basis (0.4 mm day<sup>-1</sup> in summer). However, the  
521 cooling of the western North Atlantic due to US anthropogenic aerosols also enhances the  
522 southerly flow of moist air from the Gulf of Mexico which increases cloud cover,  
523 precipitation, and soil moisture in the central US. The increase in cloud cover over the  
524 central US magnifies in turn the aerosol cooling effect. This hydrological contribution to  
525 the central US “warming hole” has been previously identified from observations by  
526 Robinson et al. (2002) and Pan et al. (2004), and we show that it is consistent with the  
527 expected effect of US anthropogenic aerosols.

528

529 We went on to examine the effect of changing US anthropogenic aerosol sources on US  
530 surface air temperatures over the 1950-2050 period, comparing to observed trends over  
531 the mid-Atlantic US where the aerosol radiative effect is strongest. Without US  
532 anthropogenic aerosol sources, we find in the model a relatively constant rate of warming  
533 over the 1950-2050 period, driven by increasing greenhouse gases. In contrast, the  
534 observations show no warming trend from 1950 to 1980, followed by very rapid warming  
535 from 1980 to present. We show that this pattern can be explained by US anthropogenic  
536 aerosol sources. The lack of warming from 1950 to 1980 reflects an increasing US  
537 aerosol loading, offsetting the warming from greenhouse gases. As the aerosol sources

538 level off in 1980 and then decrease, warming takes over and accelerates due to the loss of  
539 the aerosol cooling shield. We thus find that the observed warming from 1990 to 2010 is  
540 significantly greater than would have been expected from greenhouse gases alone. We  
541 project that future reductions in US aerosol sources will increase warming over the mid-  
542 Atlantic US by 0.1°C. However, we find that most of the warming due to reducing US  
543 aerosol sources for air quality objectives has in fact already been realized (0.35°C over  
544 the mid-Atlantic US in 1980-2010).

545

546 Our results have several implications for US air quality policy. We find that reductions in  
547 aerosol sources to improve air quality have elicited a strong regional warming response  
548 over the past 20 years. However, we also find that future aerosol reductions should have  
549 little climate impact because sources are already low. It has been suggested that future  
550 black carbon (BC) emission controls could provide relief from future warming (Bond,  
551 2007; Grieshop et al., 2009; Penner et al., 2010), but we find that BC sources in the US  
552 are too small for their climatic impact to be significant.

553

554 Although our results are specific to the US, they also warn of possibly strong regional  
555 warming over East Asia in the coming decades as China embarks on vigorous emission  
556 controls to address its pressing aerosol pollution problem. Climate response to  
557 anthropogenic aerosols in East Asia may be very different from the US because of the  
558 greater contribution of BC to the aerosol mix and because of specific meteorological  
559 features such as the monsoon. Application of our approach to that region would be of  
560 considerable interest.

561

## 562 **Acknowledgments**

563 This work was funded by the Electric Power Research Institute (EPRI) and by an EPA  
564 Science to Achieve Results (STAR) Graduate Research Fellowship to Eric  
565 Leibensperger. The EPRI and EPA has not officially endorsed this publication and the  
566 views expressed herein may not reflect those of the EPRI and EPA. This work utilized  
567 resources and technical support offered by the Harvard University School of Engineering  
568 and Applied Science (SEAS) Instructional and Research Computing Services (IRCS). We

569 would like to thank Jeff Jonas and Mark Chandler of NASA GISS for help with ocean  
570 heat flux calculations and Jack Yatteau for computational assistance.

571 **References:**

572

573 Adams, P. J., and Seinfeld, J. H.: Predicting global aerosol size distributions in general  
574 circulation models, *J Geophys Res-Atmos*, 107, 4370, doi: 10.1029/2001JD001010,  
575 2002.

576

577 Andreae, M., Jones, C., and Cox, P.: Strong present-day aerosol cooling implies a hot  
578 future, *Nature*, 435, 1187-1190, doi: 10.1038/nature03671, 2005.

579

580 Bey, I., Jacob, D., Yantosca, R., Logan, J., Field, B., Fiore, A., Li, Q., Liu, H., Mickley,  
581 L., and Schultz, M.: Global modeling of tropospheric chemistry with assimilated  
582 meteorology: Model description and evaluation, *J Geophys Res-Atmos*, 106, 23073-  
583 23095, 2001.

584

585 Bond, T. C.: Can warming particles enter global climate discussions?, *Environ Res Lett*,  
586 2, 045030, 2007.

587

588 Bond, T. C., Bhardwaj, E., Dong, R., Jogani, R., Jung, S., Roden, C., Streets, D. G., and  
589 Trautmann, N. M.: Historical emissions of black and organic carbon aerosol from energy-  
590 related combustion, 1850–2000, *Global Biogeochem Cy*, 21, GB2018, doi:  
591 10.1029/2006GB002840, 2007.

592

593 Bouwman, A., Lee, D., Asman, W., Dentener, F., Van Der Hoek, K., and Olivier, J.: A  
594 global high-resolution emission inventory for ammonia, *Global Biogeochem Cy*, 11, 561-  
595 587, 1997.

596

597 Brasseur, G., and Roeckner, E.: Impact of improved air quality on the future evolution of  
598 climate, *Geophys Res Lett*, 32, L23704, doi: 10.1029/2005GL023902, 2005.

599

600 Chang, W., Liao, H., and Wang, H.: Climate responses to direct radiative forcing of  
601 anthropogenic aerosols, tropospheric ozone, and long-lived greenhouse gases in eastern  
602 China over 1951–2000, *Adv Atmos Sci*, 26, 748-762, doi: 10.1007/s00376-009-9032-4,  
603 2009.

604

605 Chen, W.-T., Nenes, A., Liao, H., Adams, P. J., Li, J.-L. F., and Seinfeld, J. H.: Global  
606 climate response to anthropogenic aerosol indirect effects: Present day and year 2100, *J*  
607 *Geophys Res-Atmos*, 115, D12207, doi: 10.1029/2008JD011619, 2010.

608

609 Chin, M., Rood, R., Lin, S., Muller, J., and Thompson, A.: Atmospheric sulfur cycle  
610 simulated in the global model GOCART: Model description and global properties, *J*  
611 *Geophys Res-Atmos*, 105, 24671-24687, 2000.

612

613 Chung, S., and Seinfeld, J.: Global distribution and climate forcing of carbonaceous  
614 aerosols, *J Geophys Res-Atmos*, 107, 4407, doi: 10.1029/2001JD001397, 2002.  
615

616 Del Genio, A., Yao, M., Kovari, W., and Lo, K.: A prognostic cloud water  
617 parameterization for global climate models, *J Climate*, 9, 270-304, 1996.  
618

619 Duncan, B., Martin, R., Staudt, A., Yevich, R., and Logan, J.: Interannual and seasonal  
620 variability of biomass burning emissions constrained by satellite observations, *J Geophys*  
621 *Res-Atmos*, 108, 4100, doi: 10.1029/2002JD002378, 2003.  
622

623 Fiore, A. M., Jacob, D. J., Field, B. D., Streets, D. G., Fernandes, S. D., and Jang, C.:  
624 Linking ozone pollution and climate change: The case for controlling methane, *Geophys*  
625 *Res Lett*, 29, 1919, doi: 10.1029/2002GL015601, 2002.  
626

627 Fischer-Bruns, I., Banse, D. F., and Feichter, J.: Future impact of anthropogenic sulfate  
628 aerosol on North Atlantic climate, *Clim Dynam*, 32, 511-524, doi: 10.1007/s00382-008-  
629 0458-7, 2009.  
630

631 Fischer-Bruns, I., Feichter, J., Kloster, S., and Schneidereit, A.: How present aerosol  
632 pollution from North America impacts North Atlantic climate, *Tellus A*, 1-11, doi:  
633 10.1111/j.1600-0870.2010.00446.x, 2010.  
634

635 Fountoukis, C., and Nenes, A.: Continued development of a cloud droplet formation  
636 parameterization for global climate models, *J Geophys Res-Atmos*, 110, D11212, doi:  
637 10.1029/2004JD005591, 2005.  
638

639 Grieshop, A. P., Reynolds, C. C. O., Kandlikar, M., and Dowlatabadi, H.: A black-carbon  
640 mitigation wedge, *Nat Geosci*, 2, 533-534, 2009.  
641

642 Hansen, J., Fung, I., Lacis, A., Rind, D., Lebedeff, S., Ruedy, R., Russell, G., and Stone,  
643 P.: Global climate changes as forecast by Goddard Institute For Space Studies 3-  
644 dimensional model, *J Geophys Res-Atmos*, 93, 9341-9364, 1988.  
645

646 Hansen, J., Ruedy, R., Sato, M., Imhoff, M., Lawrence, W., Easterling, D., Peterson, T.,  
647 and Karl, T.: A closer look at United States and global surface temperature change, *J*  
648 *Geophys Res-Atmos*, 106, 23,947-925,963, 2001.  
649

650 Hansen, J., Sato, M., Nazarenko, L., Ruedy, R., Lacis, A., Koch, D., Tegen, I., Hall, T.,  
651 Shindell, D., Santer, B., Stone, P., Novakov, T., Thomason, L., Wang, R., Wang, Y.,  
652 Jacob, D., Hollandsworth, S., Bishop, L., Logan, J., Thompson, A., Stolarski, R., Lean, J.,  
653 Willson, R., Levitus, S., Antonov, J., Rayner, N., Parker, D., and Christy, J.: Climate  
654 forcings in Goddard Institute for Space Studies SI2000 simulations, *J Geophys Res-*  
655 *Atmos*, 107, 37, doi: 10.1029/2001JD001143, 2002.  
656

657 Hegerl, G. C., Zwiers, F. W., Braconnot, P., Gillett, N. P., Luo, Y., Marengo Orsini, J. A.,  
658 Nicholls, N., Penner, J. E., and Stott, P. A.: Understanding and Attributing Climate  
659 Change, in: *Climate Change 2007: The Physical Science Basis*, New York, NY, 2007.  
660

661 Hoose, C., Lohmann, U., Bennartz, R., Croft, B., and Lesins, G.: Global simulations of  
662 aerosol processing in clouds, *Atmos Chem Phys*, 8, 6939-6963, doi: 10.5194/acp-8-6939-  
663 2008, 2008.  
664

665 Jacobson, M. Z.: Short-term effects of agriculture on air pollution and climate in  
666 California, *J Geophys Res-Atmos*, 113, D23101, doi: 10.1029/2008JD010689, 2008.  
667

668 Jones, A., Haywood, J. M., and Boucher, O.: Aerosol forcing, climate response and  
669 climate sensitivity in the Hadley Centre climate model, *J Geophys Res-Atmos*, 112,  
670 D20211, doi: 10.1029/2007JD008688, 2007.  
671

672 Khairoutdinov, M., and Kogan, Y.: A new cloud physics parameterization in a large-eddy  
673 simulation model of marine stratocumulus, *Mon Weather Rev*, 128, 229-243, 2000.  
674

675 Kloster, S., Dentener, F., Feichter, J., Raes, F., Lohmann, U., Roeckner, E., and Fischer-  
676 Bruns, I.: A GCM study of future climate response to aerosol pollution reductions, *Clim  
677 Dyn*, 34, 1177-1194, doi: 10.1007/s00382-009-0573-0, 2009.  
678

679 Kunkel, K., Liang, X.-Z., Zhu, J., and Lin, Y.: Can CGCMs simulate the twentieth-  
680 century "warming hole" in the central United States?, *J Climate*, 19, 4137-4153, 2006.  
681

682 Lee, W., and Kim, M.: Effects of radiative forcing by black carbon aerosol on spring  
683 rainfall decrease over Southeast Asia, *Atmos Environ*, 44, 3739-3744, 2010.  
684

685 Leibensperger, E. M., Mickley, L. J., and Jacob, D. J.: Sensitivity of US air quality to  
686 mid-latitude cyclone frequency and implications of 1980-2006 climate change, *Atmos  
687 Chem Phys*, 8, 12, doi: 10.5194/acp-8-7075-2008, 2008.  
688

689 Leibensperger, E. M., Mickley, L. J., Jacob, D. J., Chen, W. T., Seinfeld, J. H., Nenes,  
690 A., Adams, P. J., Streets, D. G., Kumar, N., and Rind, D.: Climatic effects of 1950-2050  
691 changes in US anthropogenic aerosols - Part 1: Aerosol trends and radiative forcing,  
692 *Atmos Chem Phys Discuss*, submitted.  
693

694 Levy, H., Schwarzkopf, M. D., Horowitz, L., Ramaswamy, V., and Findell, K. L.: Strong  
695 sensitivity of late 21st century climate to projected changes in short-lived air pollutants, *J  
696 Geophys Res-Atmos*, 113, D06102, doi: 10.1029/2007JD009176, 2008.  
697

698 Liao, H., Seinfeld, J., Adams, P., and Mickley, L.: Global radiative forcing of coupled  
699 tropospheric ozone and aerosols in a unified general circulation model, *J Geophys Res-  
700 Atmos*, 109, D16207, doi: 10.1029/2003JD004456, 2004.  
701

702 Liao, H., Henze, D. K., Seinfeld, J. H., Wu, S., and Mickley, L. J.: Biogenic secondary  
703 organic aerosol over the United States: Comparison of climatological simulations with  
704 observations, *J Geophys Res-Atmos*, 112, D06201, doi: 10.1029/2006JD007813, 2007.  
705

706 Liepert, B., and Tegen, I.: Multidecadal solar radiation trends in the United States and  
707 Germany and direct tropospheric aerosol forcing, *J Geophys Res-Atmos*, 107, 4153, doi:  
708 10.1029/2001JD000760, 2002.  
709

710 Liu, B., Xu, M., Henderson, M., and Gong, W.: A spatial analysis of pan evaporation  
711 trends in China, 1955-2000, *J Geophys Res-Atmos*, 109, D15102, doi:  
712 10.1029/2004JD004511, 2004a.  
713

714 Liu, B., Xu, M., Henderson, M., Qi, Y., and Li, Y.: Taking China's temperature: Daily  
715 range, warming trends, and regional variations, 1955-2000, *J Climate*, 17, 4453-4462,  
716 2004b.  
717

718 Long, C. N., Dutton, E. G., Augustine, J. A., Wiscombe, W., Wild, M., Mcfarlane, S. A.,  
719 and Flynn, C. J.: Significant decadal brightening of downwelling shortwave in the  
720 continental United States, *J Geophys Res-Atmos*, 114, D00D06, doi:  
721 10.1029/2008JD011263, 2009.  
722

723 Makowski, K., Jaeger, E. B., Chiacchio, M., Wild, M., Ewen, T., and Ohmura, A.: On the  
724 relationship between diurnal temperature range and surface solar radiation in Europe, *J*  
725 *Geophys Res-Atmos*, 114, D00D07, doi: 10.1029/2008JD011104, 2009.  
726

727 Martin, G. M., Johnson, D. W., and Spice, A.: The measurement and parameterization of  
728 effective radius of droplets in warm stratocumulus clouds, *J Atmos Sci*, 51, 1823-1842,  
729 1994.  
730

731 Menon, S., Hansen, J., Nazarenko, L., and Luo, Y.: Climate effects of black carbon  
732 aerosols in China and India, *Science*, 297, 2250-2253, 2002.  
733

734 Mickley, L. J., Leibensperger, E. M., Jacob, D. J., and Rind, D.: Regional warming from  
735 aerosol removal over the United States: Results from a transient 2010-2050 climate  
736 simulation, *Atmos Environ*, submitted.  
737

738 Mitchell, J., Davis, R., Ingram, W., and Senior, C.: On surface temperature, greenhouse  
739 gases, and aerosols: Models and observations, *J Climate*, 8, 2364-2386, 1995.  
740

741 Morales, R., and Nenes, A.: Characteristic updrafts for computing distribution-averaged  
742 cloud droplet number, autoconversion rate and effective radius, *J Geophys Res*, 115,  
743 D18220, doi: 10.1029/2009JD013233, 2010.  
744

745 Nakićenović, N., and Swart, R.: Special Report on Emission Scenarios. A Special Report  
746 of the Working Group III of Intergovernmental Panel on Climate Change, in: A Special

747 Report of the Working Group III of Intergovernmental Panel on Climate Change,  
748 Cambridge University Press, Cambridge, U.K. and New York, NY USA, 569, 2000.  
749

750 Nenes, A., and Seinfeld, J.: Parameterization of cloud droplet formation in global climate  
751 models, *J Geophys Res-Atmos*, 108, 4415, doi: 10.1029/2002JD002911, 2003.  
752

753 Olivier, J. G. J., and Berdowski, J. J. M.: Global emissions sources and sinks, in: *The*  
754 *Climate System*, edited by: J. Berdowski et al., A. A. Balkema Publishers/Swets and  
755 Zeitliner Publishers, Lisse, Netherlands, 33-78, 2001.  
756

757 Pan, Z. T., Arritt, R. W., Takle, E. S., Gutowski, W. J., Anderson, C. J., and Segal, M.:  
758 Altered hydrologic feedback in a warming climate introduces a "warming hole", *Geophys*  
759 *Res Lett*, 31, L17109, doi: 10.1029/2004GL020528, 2004.  
760

761 Park, R., Jacob, D., Field, B., Yantosca, R., and Chin, M.: Natural and transboundary  
762 pollution influences on sulfate-nitrate-ammonium aerosols in the United States:  
763 Implications for policy, *J Geophys Res-Atmos*, 109, D15204, doi:  
764 10.1029/2003JD004473, 2004.  
765

766 Park, R., Jacob, D., Kumar, N., and Yantosca, R.: Regional visibility statistics in the  
767 United States: Natural and transboundary pollution influences, and implications for the  
768 Regional Haze Rule, *Atmos Environ*, 40, 5405-5423, doi:  
769 10.1016/j.atmosenv.2006.04.059, 2006.  
770

771 Penner, J. E., Prather, M. J., Isaksen, I. S. A., Fugelstvedt, J. S., Klimont, Z., and  
772 Stevenson, D. S.: Short-lived uncertainty?, *Nat Geosci*, 3, 587-588, 2010.  
773

774 Peterson, T., Golubev, V. S., and Groisman, P. Y.: Evaporation Losing its Strength,  
775 *Nature*, 377, 687-688, 1995.  
776

777 Philipona, R., Behrens, K., and Ruckstuhl, C.: How declining aerosols and rising  
778 greenhouse gases forced rapid warming in Europe since the 1980s, *Geophys Res Lett*, 36,  
779 L02806, doi: 10.1029/2008GL036350, 2009.  
780

781 Pierce, J., and Adams, P.: Global evaluation of CCN formation by direct emission of sea  
782 salt and growth of ultrafine sea salt, *J Geophys Res-Atmos*, 111, D06203, doi:  
783 10.1029/2005JD006186, 2006.  
784

785 Pye, H. O. T., Liao, H., Wu, S., Mickley, L. J., Jacob, D. J., Henze, D. K., and Seinfeld, J.  
786 H.: Effect of changes in climate and emissions on future sulfate-nitrate-ammonium  
787 aerosol levels in the United States, *J Geophys Res-Atmos*, 114, D01205, doi:  
788 10.1029/2008JD010701, 2009.  
789

790 Qian, Y., and Giorgi, F.: Regional climatic effects of anthropogenic aerosols? The case of  
791 Southwestern China, *Geophys Res Lett*, 27, 3521-3524, 2000.  
792

793 Raes, F., and Seinfeld, J. H.: New Directions: Climate change and air pollution  
794 abatement: A bumpy road, *Atmos Environ*, 43, 5132-5133, doi:  
795 10.1016/j.atmosenv.2009.06.001, 2009.  
796  
797 Rayner, N., Parker, D., Horton, E., Folland, C., Alexander, L., Rowell, D., Kent, E., and  
798 Kaplan, A.: Global analyses of sea surface temperature, sea ice, and night marine air  
799 temperature since the late nineteenth century, *J Geophys Res-Atmos*, 108, 4407, doi:  
800 10.1029/2002JD002670, 2003.  
801  
802 Rind, D., Lerner, J., Jonas, J., and Mclinden, C.: Effects of resolution and model physics  
803 on tracer transports in the NASA Goddard Institute for Space Studies general circulation  
804 models, *J Geophys Res-Atmos*, 112, D09315, doi: 10.1029/2006JD007476, 2007.  
805  
806 Rind, D., Lean, J., Lerner, J., Lonergan, P., and Leboissitier, A.: Exploring the  
807 stratospheric/tropospheric response to solar forcing, *J Geophys Res-Atmos*, 113, D24103,  
808 doi: 10.1029/2008JD010114, 2008.  
809  
810 Rind, D., Jonas, J., Stammerjohn, S., and Lonergan, P.: The Antarctic ozone hole and the  
811 Northern Annular Mode: A stratospheric interhemispheric connection, *Geophys Res Lett*,  
812 36, L09818, doi: 10.1029/2009GL037866, 2009a.  
813  
814 Rind, D., Lerner, J., Mclinden, C., and Perlwitz, J.: Stratospheric ozone during the Last  
815 Glacial Maximum, *Geophys Res Lett*, 36, L09712, doi: 10.1029/2009GL037617, 2009b.  
816  
817 Robinson, W. A., Reudy, R., and Hansen, J. E.: General circulation model simulations of  
818 recent cooling in the east-central United States, *J Geophys Res-Atmos*, 107, 4748-4761,  
819 doi: 10.1029/2001JD001577, 2002.  
820  
821 Robock, A., Mu, M., Vinnikov, K., Trofimova, I., and Adamenko, T.: Forty-five years of  
822 observed soil moisture in the Ukraine: No summer desiccation (yet), *Geophys Res Lett*,  
823 32, L03401, doi: 10.1029/2004GL021914, 2005.  
824  
825 Roderick, M. L., Rotstayn, L. D., Farquhar, G. D., and Hobbins, M. T.: On the attribution  
826 of changing pan evaporation, *Geophys Res Lett*, 34, L17403, doi:  
827 10.1029/2007GL031166, 2007.  
828  
829 Ruckstuhl, C., Philipona, R., Behrens, K., Collaud Coen, M., Dürr, B., Heimo, A.,  
830 Mätzler, C., Nyeki, S., Ohmura, A., Vuilleumier, L., Weller, M., Wehrli, C., and Zelenka,  
831 A.: Aerosol and cloud effects on solar brightening and the recent rapid warming,  
832 *Geophys Res Lett*, 35, L12708, doi: 10.1029/2008GL034228, 2008.  
833  
834 Schmidt, G., Ruedy, R., Hansen, J., Aleinov, I., Bell, N., Bauer, M., Bauer, S., Cairns, B.,  
835 Canuto, V., Cheng, Y., Del Genio, A., Faluvegi, G., Friend, A., Hall, T., Hu, Y., Kelley,  
836 M., Kiang, N., Koch, D., Lacis, A., Lerner, J., Lo, K., Miller, R., Nazarenko, L., Oinas,  
837 V., Perlwitz, J., Perlwitz, J., Rind, D., Romanou, A., Russell, G., Sato, M., Shindell, D.,  
838 Stone, P., Sun, S., Tausnev, N., Thresher, D., and Yao, M.: Present-day atmospheric

839 simulations using GISS ModelE: Comparison to in situ, satellite, and reanalysis data, *J*  
840 *Climate*, 19, 153-192, 2006.

841

842 Schulz, M., Textor, C., Kinne, S., Balkanski, Y., Bauer, S., Bernsten, T., Berglen, T.,  
843 Boucher, O., Dentener, F., and Guibert, S.: Radiative forcing by aerosols as derived from  
844 the AeroCom present-day and pre-industrial simulations, *Atmos Chem Phys*, 6, 5225-  
845 5246, doi: 10.5194/acp-6-5225-2006, 2006.

846

847 Shindell, D. T., Faluvegi, G., Bauer, S. E., Koch, D. M., Unger, N., Menon, S., Miller, R.  
848 L., Schmidt, G. A., and Streets, D. G.: Climate response to projected changes in short-  
849 lived species under an A1B scenario from 2000-2050 in the GISS climate model, *J*  
850 *Geophys Res-Atmos*, 112, D20103, doi: 10.1029/2007JD008753, 2007.

851

852 Shindell, D. T., Levy, H., Schwarzkopf, M. D., Horowitz, L. W., Lamarque, J.-F., and  
853 Faluvegi, G.: Multimodel projections of climate change from short-lived emissions due to  
854 human activities, *J Geophys Res-Atmos*, 113, D11109, doi: 10.1029/2007JD009152,  
855 2008.

856

857 Streets, D., Bond, T., Carmichael, G., Fernandes, S., Fu, Q., He, D., Klimont, Z., Nelson,  
858 S., Tsai, N., Wang, M., Woo, J., and Yarber, K.: An inventory of gaseous and primary  
859 aerosol emissions in Asia in the year 2000, *J Geophys Res-Atmos*, 108, 8809, doi:  
860 10.1029/2002JD003093, 2003.

861

862 Streets, D., Bond, T., Lee, T., and Jang, C.: On the future of carbonaceous aerosol  
863 emissions, *J Geophys Res-Atmos*, 109, D24212, doi: 10.1029/2004JD004902, 2004.

864

865 Streets, D. G., Yan, F., Chin, M., Diehl, T., Mahowald, N., Schultz, M., Wild, M., Wu,  
866 Y., and Yu, C.: Anthropogenic and natural contributions to regional trends in aerosol  
867 optical depth, 1980-2006, *J Geophys Res-Atmos*, 114, D00D18, doi:  
868 10.1029/2008JD011624, 2009.

869

870 Sun, S., and Hansen, J. E.: Climate simulations for 1951-2050 with a coupled  
871 atmosphere-ocean model, *J Climate*, 16, 2807-2826, 2003.

872

873 Trenberth, K. E., Jones, P. D., Ambenje, P., Bojariu, R., Easterling, D., Klein Tank, A.,  
874 Parker, D., Rahimzadeh, F., Renwick, J. A., Rusticucci, M., Soden, B., and Zhai, P.:  
875 Observations: Surface and Atmospheric Climate Change, in: *Climate Change 2007: The*  
876 *Physical Science Basis*, New York, NY, 2007.

877

878 US Environmental Protection Agency: *Our Nation's Air - Status and Trends through*  
879 *2008*, Washington, DC, 2010.

880

881 van Aardenne, J., Dentener, F., and Olivier, J.: A 1°x1° resolution data set of historical  
882 anthropogenic trace gas emissions for the period 1890–1990, *Global Biogeochem Cy*, 15,  
883 909-928, 2001.

884

885 Wang, C., Kim, D., Ekman, A. M. L., Barth, M. C., and Rasch, P. J.: Impact of  
886 anthropogenic aerosols on Indian summer monsoon, *Geophys Res Lett*, 36, L21704, doi:  
887 10.1029/2009GL040114, 2009a.  
888

889 Wang, H., Schubert, S., Suarez, M., Chen, J., Hoerling, M., Kumar, A., and Pegen, P.:  
890 Attribution of the seasonality and regionality in climate trends over the United States  
891 during 1950-2000, *J Climate*, 22, 2571-2590, 2009b.  
892

893 Wang, Y., Jacob, D., and Logan, J.: Global simulation of tropospheric O<sub>3</sub>-NO<sub>x</sub>-  
894 hydrocarbon chemistry 1. Model formulation, *J Geophys Res-Atmos*, 103, 10713-10725,  
895 1998.  
896

897 Wild, M., Ohmura, A., and Makowski, K.: Impact of global dimming and brightening on  
898 global warming, *Geophys Res Lett*, 34, L04702, doi: 10.1029/2006GL028031, 2007.  
899

900 Wild, M.: How well do IPCC-AR4/CMIP3 climate models simulate global  
901 dimming/brightening and twentieth-century daytime and nighttime warming?, *J Geophys*  
902 *Res-Atmos*, 114, D00D11, doi: 10.1029/2008JD011372, 2009a.  
903

904 Wild, M.: Global dimming and brightening: A review, *J Geophys Res-Atmos*, 114,  
905 D00D16, doi: 10.1029/2008JD011470, 2009b.  
906

907 Wu, S., Mickley, L. J., Leibensperger, E. M., Jacob, D. J., Rind, D., and Streets, D. G.:  
908 Effects of 2000-2050 global change on ozone air quality in the United States, *J Geophys*  
909 *Res-Atmos*, 113, D06302, doi: 10.1029/2007JD008917, 2008.  
910

911 Zhang, Y., Sun, S., Olsen, S. C., Dubey, M. K., and He, J.: CCSM3 simulated regional  
912 effects of anthropogenic aerosols for two contrasting scenarios: rising Asian emissions  
913 and global reduction of aerosols, *Int J Climatol*, doi: 10.1002/joc.2060, 2009.  
914

915 Zwiers, F., and von Storch, H.: Taking serial correlation into account in tests of the mean,  
916 *J Climate*, 8, 336-351, 1995.  
917  
918  
919  
920

920 **Table 1 – Trends in surface air temperature ( $^{\circ}\text{C decade}^{-1}$ ) in the mid-Atlantic US<sup>a</sup>**

	<b>1960-1979</b>	<b>1980-2010</b>	<b>2020-2050</b>
Observations <sup>b</sup>	+0.01 $\pm$ 0.20 <sup>c</sup>	+0.21 $\pm$ 0.18	---
Model			
Control <sup>d</sup>	-0.02 $\pm$ 0.20	+0.41 $\pm$ 0.08	+0.29 $\pm$ 0.07
No US Anthropogenic Aerosols <sup>e</sup>	+0.30 $\pm$ 0.19	+0.30 $\pm$ 0.10	+0.25 $\pm$ 0.08

921

922 <sup>a</sup> Averages for the boxed region in Fig. 2

923 <sup>b</sup> Observations from the NASA GISS Surface Temperature Analysis (GISTEMP;  
 924 <http://data.giss.nasa.gov/gistemp/>)

925 <sup>c</sup> 95% confidence interval

926 <sup>d</sup> Control simulation including best estimates of greenhouse gas, aerosol, and natural  
 927 radiative forcing

928 <sup>e</sup> Sensitivity simulation excluding US anthropogenic sources of SO<sub>2</sub>, NO<sub>x</sub>, black  
 929 carbon (BC), and primary organic aerosol (POA)

930

931

931 **Figure Captions**

932 **Figure 1** – Observed change in surface air temperature between 1930 and 1990.

933 Temperature change is based on the linear trend as in Hansen et al. (2001). Observations  
934 are from the NASA GISS Surface Temperature Analysis (GISTEMP;  
935 <http://data.giss.nasa.gov/gistemp/>).

936 **Figure 2** – Changes in net top-of-atmosphere (TOA) radiation (left) and surface solar  
937 radiation (right) due to US anthropogenic aerosol sources. The top panels show the  
938 annual mean aerosol effect (direct and indirect) averaged over 1970-1990. The bottom  
939 panels show the 1950-2050 evolution of the direct effect only (dashed) and the sum of  
940 direct and indirect effects (solid) averaged over the mid-Atlantic US (boxed region).

941 Values are differences between the control simulation and a simulation with US  
942 anthropogenic aerosol sources shut off. In the top panels, dots indicate differences  
943 significant at the 95<sup>th</sup> percentile, downward triangles indicate observation sites used by  
944 Liepert and Tegen (2002), and upward triangles indicate observation sites used by Long  
945 et al. (2009). In the lower panels, black squares indicate the annual mean aerosol direct  
946 radiative forcings over the mid-Atlantic US region from US anthropogenic sources  
947 calculated by Leibensperger et al. (2011). Time series have been filtered by a 15-year  
948 moving average.

949 **Figure 3** – Effect of US anthropogenic aerosol sources on annual mean temperatures (°C)  
950 for the 1970-1990 period (when US aerosol loading was at its peak). Values are shown  
951 for surface air (bottom) and 500 hPa (top) temperatures. They represent the mean  
952 difference between 5-member ensemble GCM simulations including vs. excluding US  
953 anthropogenic aerosol sources, and considering both aerosol direct and indirect effects.  
954 Dots indicate differences significant at the 95<sup>th</sup> percentile.

955 **Figure 4** – Effect of US anthropogenic aerosol sources on surface air temperatures for the  
956 1970-1990 period when US aerosol loading was at its peak. Values represent the mean  
957 difference between 5-member ensemble GCM simulations including vs. excluding US  
958 anthropogenic aerosol sources, and considering the aerosol direct only (top) and the sum  
959 of direct and indirect effects (bottom). Dots indicate differences significant at the 95<sup>th</sup>  
960 percentile. The bottom panel contains the same information as the bottom panel of Fig. 3  
961 but zoomed over the US.

962 **Figure 5** – Effect of US anthropogenic aerosols on seasonal surface air temperature  
963 statistics over the mid-Atlantic US (boxed region in Fig. 2). Values are for 1970-1990,  
964 when US aerosol loads were at their peak. Statistics were obtained by difference between  
965 5-member ensemble GCM simulations including vs. excluding US anthropogenic aerosol  
966 sources, and considering both the aerosol direct and indirect effects. Error bars indicate  
967 95% confidence intervals.

968 **Figure 6** – Effect of US anthropogenic aerosols on annual mean evaporation,  
969 precipitation, cloud cover, and soil moisture availability for the 1970-1990 period. Values  
970 represent the mean differences between 5-member ensemble GCM simulations including  
971 vs. excluding US anthropogenic aerosol sources, and considering both the aerosol direct  
972 and indirect effects. Cloud cover change and soil moisture availability are shown as  
973 absolute percentages. Changes significant at the 95<sup>th</sup> percentile are marked with a dot.

974 **Figure 7** – Change in the summer mean 850 hPa geopotential height due to US  
975 anthropogenic aerosols for the 1970-1990 period. Values represent the mean difference  
976 between 5-member ensemble GCM simulations including vs. excluding US  
977 anthropogenic aerosol sources, and considering both the aerosol direct and indirect  
978 effects. Changes significant at the 95<sup>th</sup> percentile are marked with a dot.

979 **Figure 8** – Change in annual mean surface air temperature over the mid-Atlantic US  
980 (boxed region in Fig. 2) due to US anthropogenic aerosol sources. Values are differences  
981 for 5-member ensembles between a 1950-2050 control simulation including radiative  
982 forcing from both greenhouse gases and aerosols (direct and indirect effects) and a  
983 sensitivity simulation with US anthropogenic aerosol sources shut off. The time series  
984 has been smoothed with a 15-year moving average. Shading indicates the 95%  
985 confidence interval.

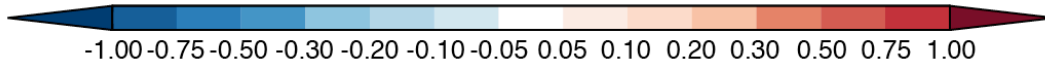
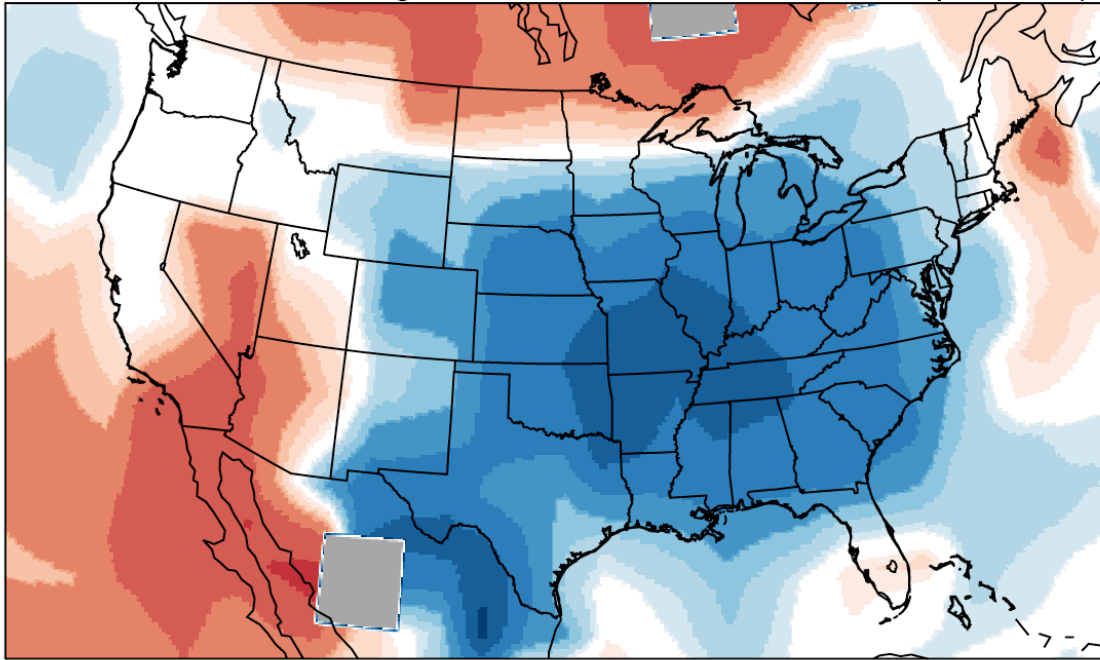
986 **Figure 9** – 1950-2050 trends in annual mean surface air temperatures over the mid-  
987 Atlantic US (boxed region in Fig. 2). Observations (GISTEMP) are compared to the  
988 control simulation including greenhouse and aerosol forcings and to the sensitivity  
989 simulation with no US anthropogenic aerosols. Observations are the anomaly relative to  
990 the observed 1951-1980 mean and are shown for individual years (thin line) and for a 15-  
991 year moving average (thick line). Model temperatures are the 5-member ensemble mean

992 anomaly relative to the 1951-1980 mean of the control simulation, and are shown as 15-  
993 year moving averages.

994

995

Observed 1930-1990 Change in Annual Mean Surface Air Temperature (°C)



995

996

997

998

999

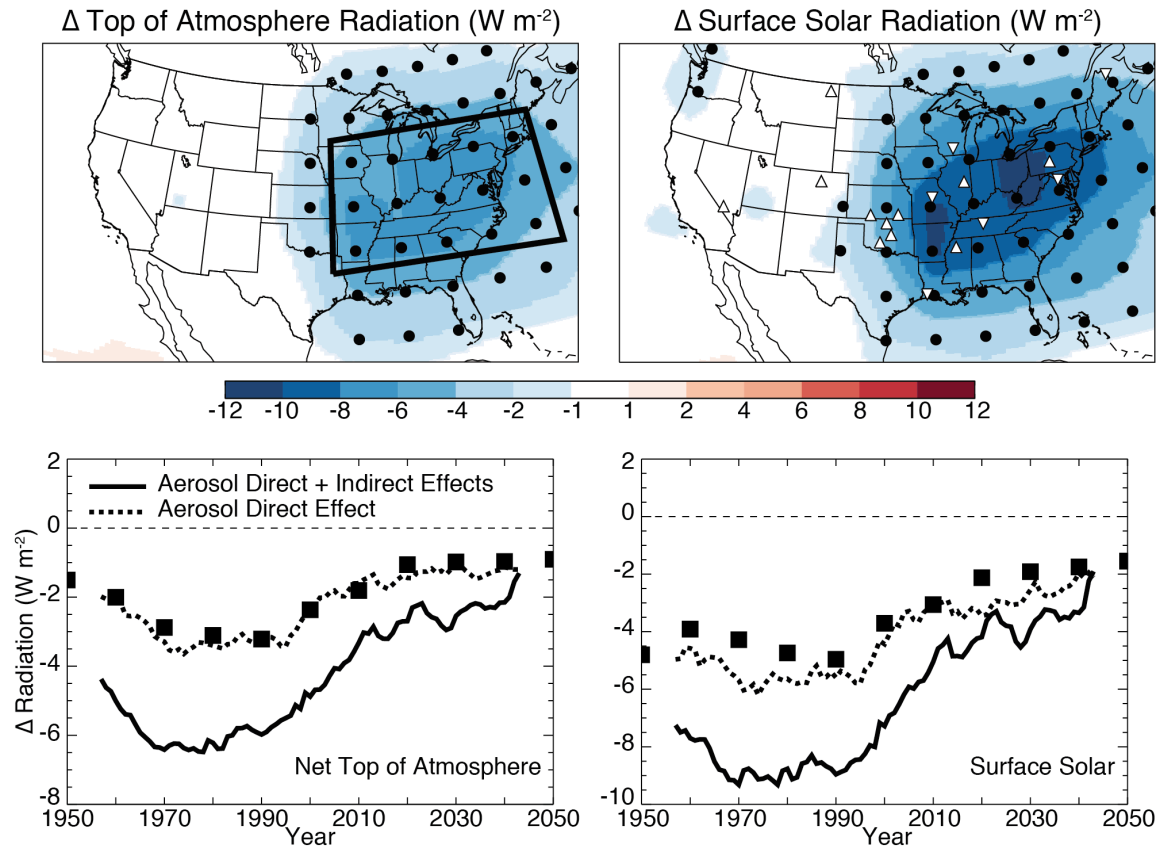
1000

**Figure 1 – Observed change in surface air temperature between 1930 and 1990.**

**Temperature change is based on the linear trend as in Hansen et al. (2001).**

**Observations are from the NASA GISS Surface Temperature Analysis (GISTEMP;**

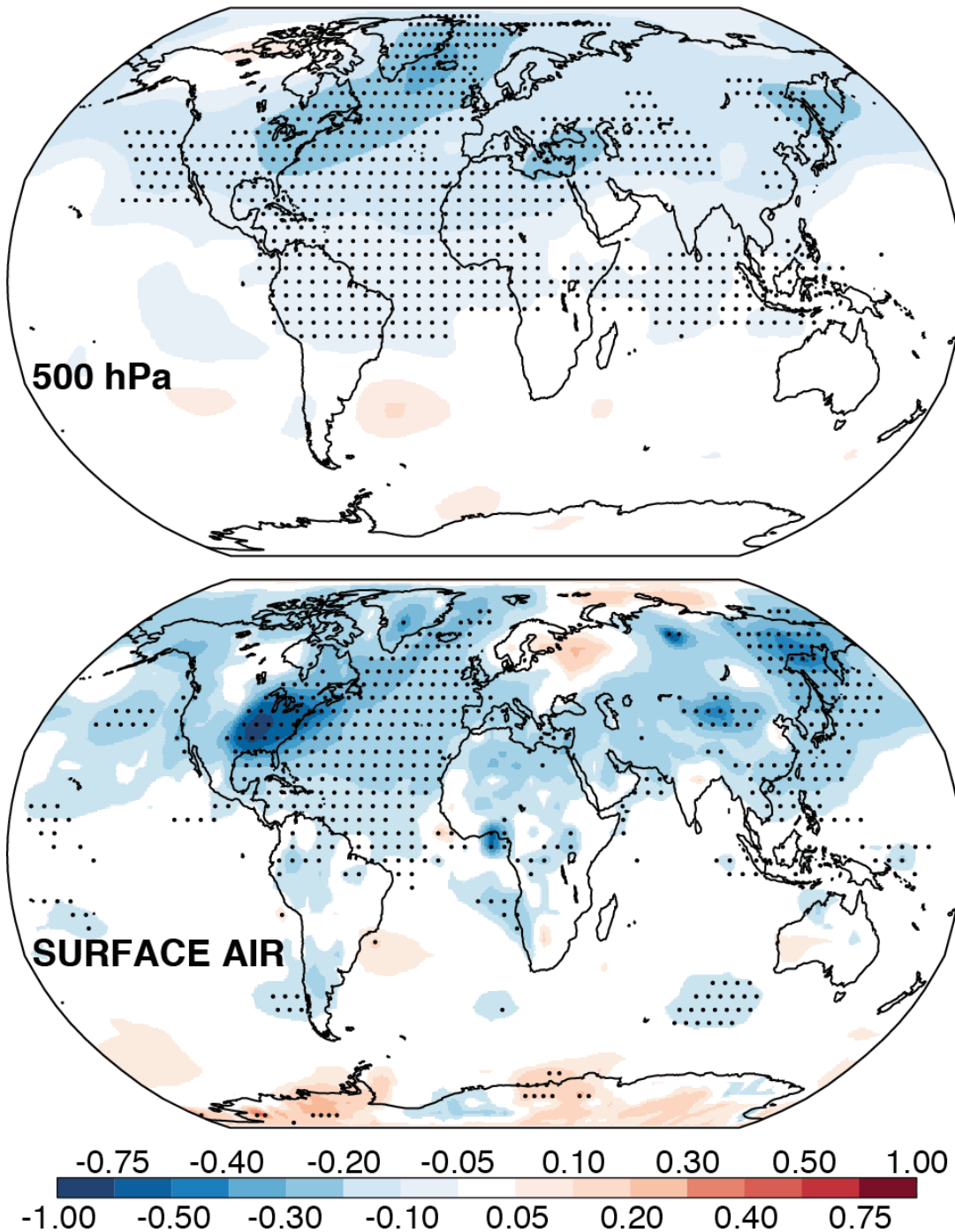
**<http://data.giss.nasa.gov/gistemp/>).**



1000  
 1001  
 1002  
 1003  
 1004  
 1005  
 1006  
 1007  
 1008  
 1009  
 1010  
 1011  
 1012  
 1013  
 1014

**Figure 2 – Changes in net top-of-atmosphere (TOA) radiation (left) and surface solar radiation (right) due to US anthropogenic aerosol sources. The top panels show the annual mean aerosol effect (direct and indirect) averaged over 1970-1990. The bottom panels show the 1950-2050 evolution of the direct effect only (dashed) and the sum of direct and indirect effects (solid) averaged over the mid-Atlantic US (boxed region). Values are differences between the control simulation and a simulation with US anthropogenic aerosol sources shut off. In the top panels, dots indicate differences significant at the 95<sup>th</sup> percentile, downward triangles indicate observation sites used by Liepert and Tegen (2002), and upward triangles indicate observation sites used by Long et al. (2009). In the lower panels, black squares indicate the annual mean aerosol direct radiative forcings over the mid-Atlantic US region from US anthropogenic sources calculated by Leibensperger et al. (submitted). Time series have been filtered by a 15-year moving average.**

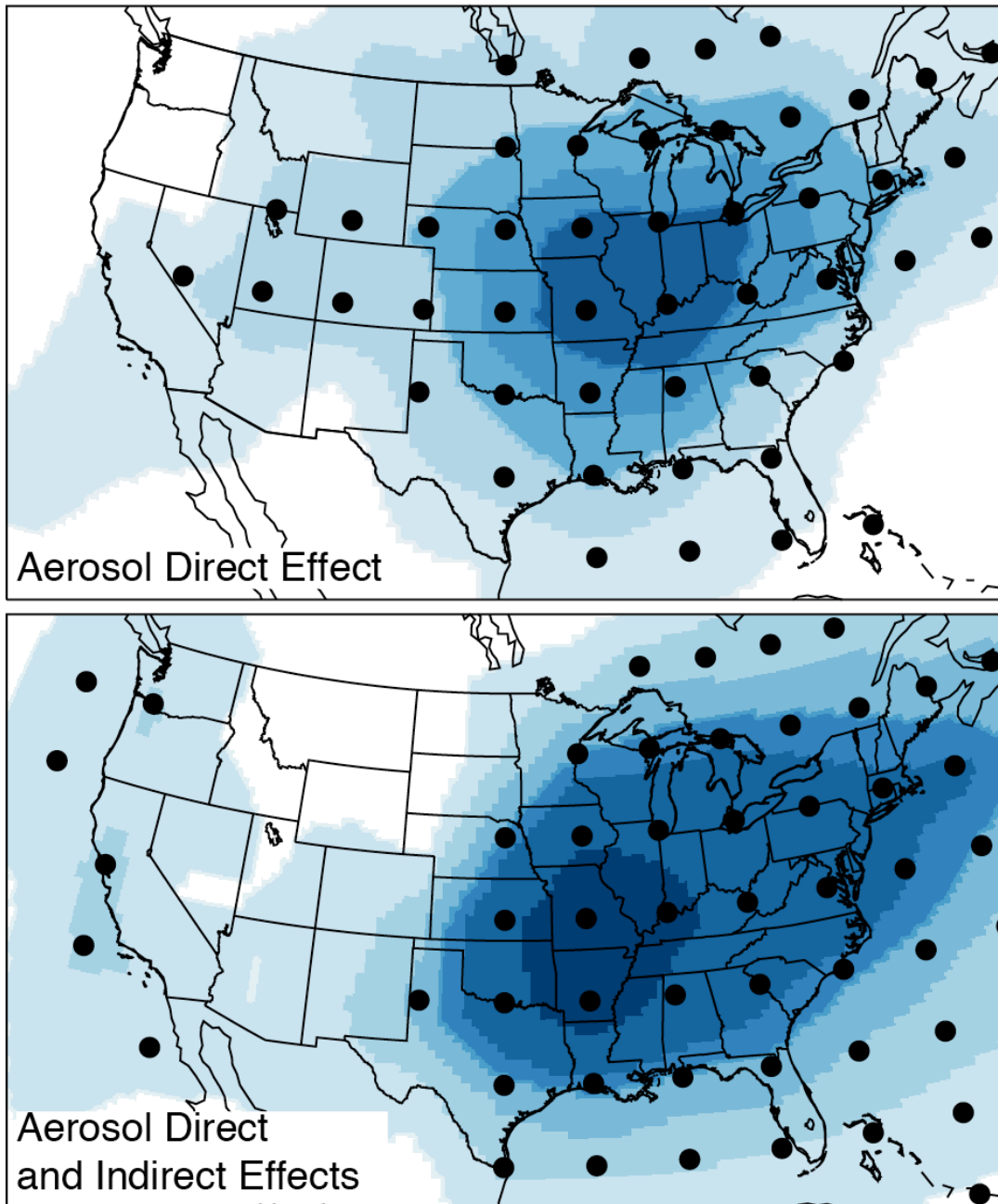
### Change in Annual Mean Temperature (°C)



1014  
1015  
1016  
1017  
1018  
1019  
1020  
1021

**Figure 3 – Effect of US anthropogenic aerosol sources on annual mean temperatures (°C) for the 1970-1990 period (when US aerosol loading was at its peak). Values are shown for surface air (bottom) and 500 hPa (top) temperatures. They represent the mean difference between 5-member ensemble GCM simulations including vs. excluding US anthropogenic aerosol sources, and considering both aerosol direct and indirect effects. Dots indicate differences significant at the 95<sup>th</sup> percentile.**

## Change in Annual Mean Surface Air Temperature (°C)

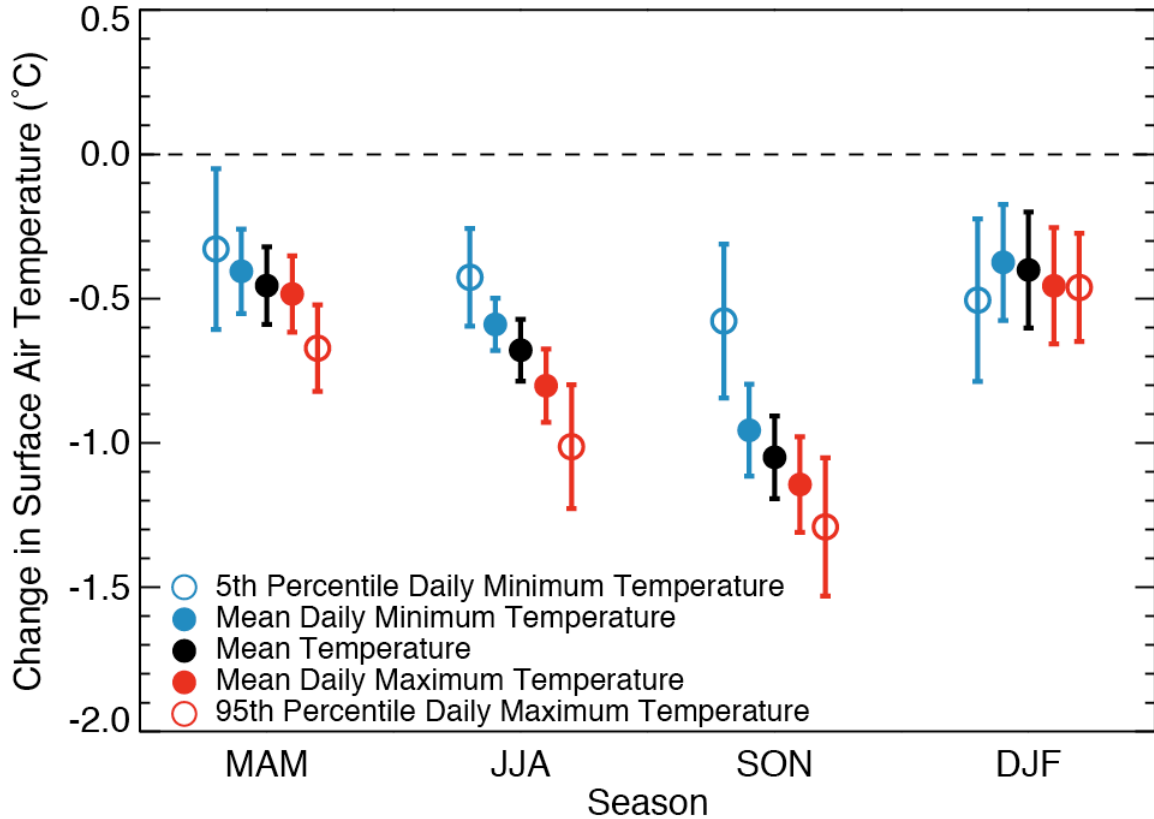


-1.00 -0.75 -0.50 -0.40 -0.30 -0.20 -0.10 0.10 0.20 0.30 0.40 0.50 0.75 1.00

1021  
1022  
1023  
1024  
1025  
1026

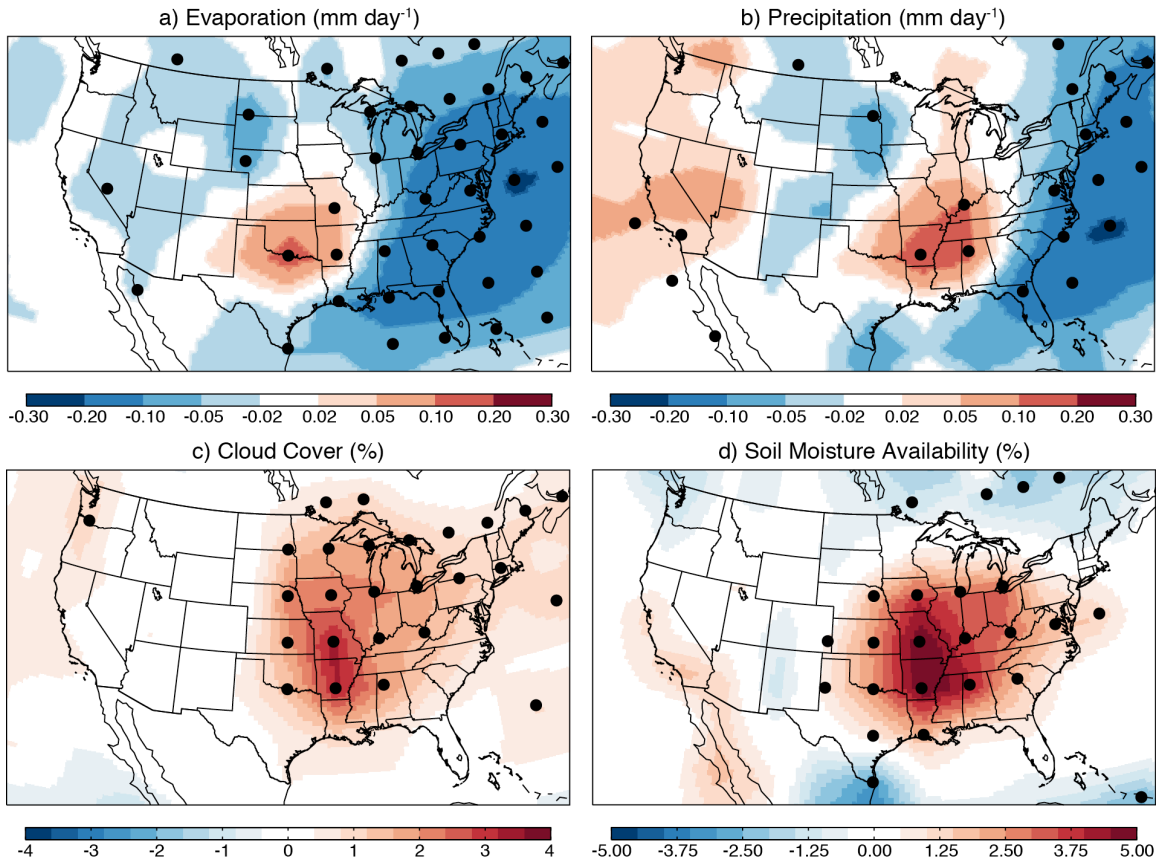
**Figure 4 – Effect of US anthropogenic aerosol sources on surface air temperatures for the 1970-1990 period when US aerosol loading was at its peak. Values represent the mean difference between 5-member ensemble GCM simulations including vs. excluding US anthropogenic aerosol sources, and considering the aerosol direct only (top) and the sum of direct and indirect effects (bottom). Dots indicate differences**

1027 **significant at the 95<sup>th</sup> percentile. The bottom panel contains the same information as**  
1028 **the bottom panel of Fig. 3 but zoomed over the US.**  
1029



1029  
 1030  
 1031  
 1032  
 1033  
 1034  
 1035  
 1036  
 1037

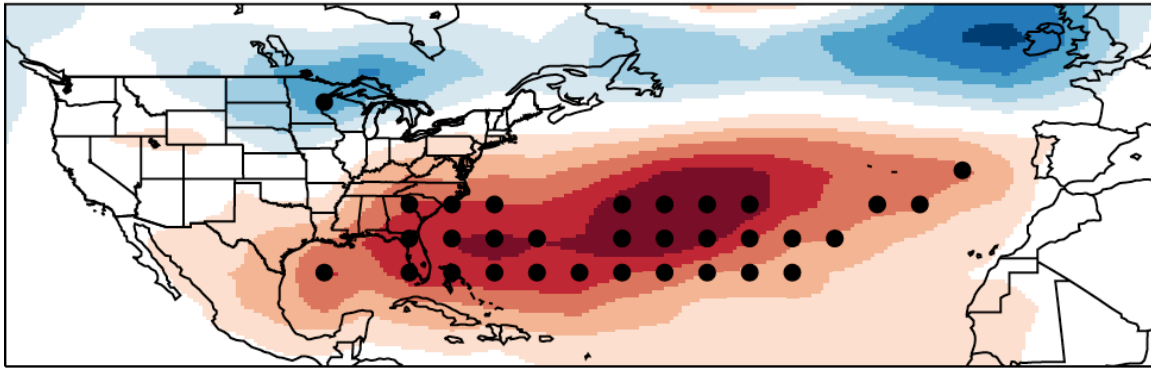
**Figure 5 - Effect of US anthropogenic aerosols on seasonal surface air temperature statistics over the mid-Atlantic US (boxed region in Fig. 2). Values are for 1970-1990, when US aerosol loads were at their peak. Statistics were obtained by difference between 5-member ensemble GCM simulations including vs. excluding US anthropogenic aerosol sources, and considering both the aerosol direct and indirect effects. Error bars indicate 95% confidence intervals.**



1037  
 1038  
 1039  
 1040  
 1041  
 1042  
 1043  
 1044  
 1045

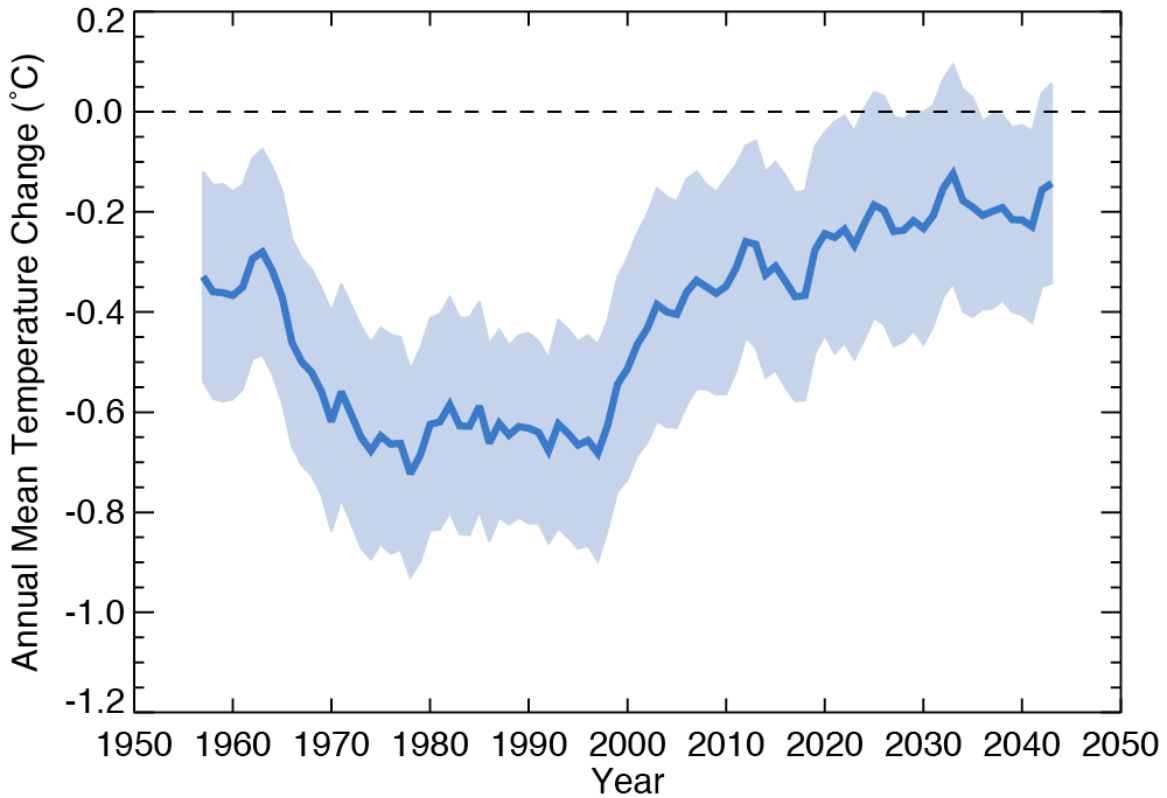
**Figure 6 – Effect of US anthropogenic aerosols on annual mean evaporation, precipitation, cloud cover, and soil moisture availability for the 1970-1990 period. Values represent the mean differences between 5-member ensemble GCM simulations including vs. excluding US anthropogenic aerosol sources, and considering both the aerosol direct and indirect effects. Cloud cover change and soil moisture availability are shown as absolute percentages. Changes significant at the 95<sup>th</sup> percentile are marked with a dot.**

Change in 850 hPa Geopotential Height (m)



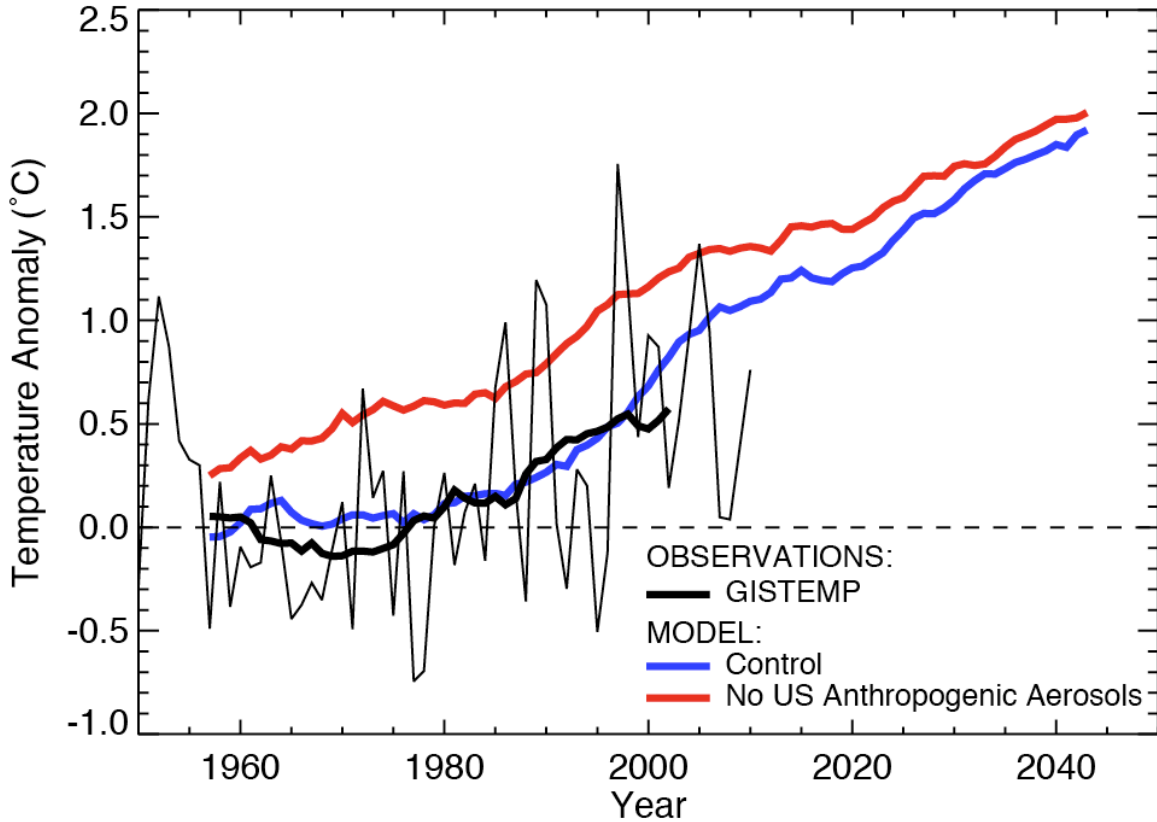
1045  
1046  
1047  
1048  
1049  
1050  
1051

**Figure 7 – Change in the summer mean 850 hPa geopotential height due to US anthropogenic aerosols for the 1970-1990 period. Values represent the mean difference between 5-member ensemble GCM simulations including vs. excluding US anthropogenic aerosol sources, and considering both the aerosol direct and indirect effects. Changes significant at the 95<sup>th</sup> percentile are marked with a dot.**



1051  
 1052  
 1053  
 1054  
 1055  
 1056  
 1057  
 1058  
 1059

**Figure 8 – Change in annual mean surface air temperature over the mid-Atlantic US (boxed region in Fig. 2) due to US anthropogenic aerosol sources. Values are differences for 5-member ensembles between a 1950-2050 control simulation including radiative forcing from both greenhouse gases and aerosols (direct and indirect effects) and a sensitivity simulation with US anthropogenic aerosol sources shut off. The time series has been smoothed with a 15-year moving average. Shading indicates the 95% confidence interval.**



1059  
 1060  
 1061  
 1062  
 1063  
 1064  
 1065  
 1066  
 1067  
 1068

**Figure 9 – 1950-2050 trends in annual mean surface air temperatures over the mid-Atlantic US (boxed region in Fig. 2). Observations (GISTEMP) are compared to the control simulation including greenhouse and aerosol forcings and to the sensitivity simulation with no US anthropogenic aerosols. Observations are the anomaly relative to the observed 1951-1980 mean and are shown for individual years (thin line) and for a 15-year moving average (thick line). Model temperatures are the 5-member ensemble mean anomaly relative to the 1951-1980 mean of the control simulation, and are shown as 15-year moving averages.**